Modeling Contagion and Systemic Risk*

Daniele Bianchi† Monica Billio‡ Roberto Casarin‡ Massimo Guidolin§

Abstract

We take a Bayesian perspective and provide a novel methodology to make robust system-wide inference on uncertain, time-varying, cross-firm financial linkages. We use this framework to investigate contagion and systemic risk within the S&P100 blue chips, and find that firms interconnectedness increased across the period 1999/2003 (e.g. Gramm-Leach-Bliley act, financial scandals, etc.), and the great financial crisis. The empirical analysis shows that firm-level network centrality does not depend on market values, while is positively correlated with financial losses. Further, we show that systemic risk partly correlates with the business cycle and with exposures to sources of systematic risks.

Keywords: Bayesian Econometrics, Markov Regime-Switching, Graphical Models, Systemic Risk, Network Connectivity

JEL codes: C11, C32, C58

*This version: September 11, 2015. We are grateful to Sönke M. Bartram, Giacomo Bormetti, Christian Brownlees, Svetlana Borovkova (discussant), Massimiliano Caporin, Antoniou Constantinos, Fulvio Corsi, Francis X. Diebold, Sylvia Frühwirth-Schnatter, Roman Kozhan, Peter Kondor, Siam J. Koopman, Daniele Massacci, Mao Lei, Fabrizio Lillo, Neil Pearson, Vikas Raman, Francesco Ravazzolo, Onur Tosun, Kamil Yilmaz, for their helpful comments and suggestions. We also thank seminar participants at the Warwick Business School, University Cá Foscari of Venice, Bocconi University, Scuola Normale Superiore di Pisa, the NBER Summer Institute 2015, the 8th Annual SoFiE conference, the SYRTO Conference on Systemic Risk, the 2nd Vienna Workshop on High-Dimensional Time Series in Macroeconomics and Finance, the 23rd Symposium of the Society for Nonlinear Dynamics and Econometrics, and the Bologna IFCS Meeting 2015. Monica Billio and Roberto Casarin acknowledge financial support from the European Union, Seventh Framework Programme FP7/2007-2013 under grant agreement SYRTO-SSH-2012-320270, from the Institut Europlace de Finance under the *Systemic Risk* grant, and from the Italian Ministry of Education, University and Research (MIUR) PRIN 2010-11 grant MISURA.

†Warwick Business School, University of Warwick, Coventry, UK. Daniele.Bianchi@wbs.ac.uk

‡Department of Economics, University Cá Foscari of Venice, Venice, Italy

§Department of Finance and IGIER, Bocconi University, Milan, Italy.

1 Introduction

The financial crisis of 2007/2009 has shown that liquidity shocks, insolvency, and losses can quickly propagate affecting institutions in different markets, with different sizes and structures. Investigate how cross-firm linkages evolve over time is therefore of first order importance for contagion and systemic risk management purposes. Surprisingly, however, cross-firm connectivity remains a rather elusive concept, in many respects poorly identified and empirically measured in dynamic contexts.[1]

In this paper, we address this issue by taking an asset pricing perspective and develop a unifying framework to identify cross-firm connectedness in large dimensional time series settings, where systematic and systemic risks are not mutually exclusive. Our methodology directly refers to the concept of networks. Network analysis is omnipresent in modern life, from Twitter to the study of the transmission of virus diseases. Broadly speaking, a network represents the interconnections of a large multivariate system, and its graph representation can be used to study the properties of the transmission mechanism of a shock (e.g. patient zero). We remain agnostic as to how network connectivity arises; rather, we take it as given and seek how to capture it correctly for systemic risk measurement purposes.

For a given linear factor pricing model, we model contagion and systemic risk as a shift in the strength of cross-firm network linkages, which are inferred system-wide from the covariance structure of the model residuals. This is consistent with the common definition of contagion as a significant and potentially persistent jump in cross-sectional correlations (see Forbes and Rigobon 2000). Also, by looking at the model residuals, we allow systematic and systemic risks to coexist, such that firm-specific exposures to sources of systematic risks directly depend on the level of aggregate network connectivity.

This paper builds on a recent literature advocating the use of network analysis in economics and finance to make inference on the connectedness of institutions, sectors and countries,

[1] See among others Forbes and Rigobon (2000), Forbes and Rigobon (2002) and Corsetti, Pericoli, and Sbracia (2005), Adrian and Brunnermeier (2010), Acharya, Pedersen, Phillippon, and Richardson (2011), Corsetti, Pericoli, and Sbracia (2011), Billio, Getmansky, Lo, and Pelizzon (2012), Bekaert, Ehrmann, Fratzscher, and Mehl (2014), Barigozzi and Brownlees (2014), Diebold and Yilmaz (2014), Brownlees and Engle (2015), Giglio, Kelly, and Pruitt (2015) just to cite a few.

such as Allen and Gale (2000), Goyal (2007), Jackson (2008), Easley and Kleinberg (2010), Billio et al. (2012), Hautsch, Schaumburg, and Schienle (2012), Ahren and Harford (2014), Barigozzi and Brownlees (2014), Diebold and Yilmaz (2014),Timmermann, Blake, Tonks, and Rossi (2014), Brownlees, Nualart, and Sun (2014), Ahern (2015), and Diebold and Yilmaz (2015). In particular, Billio et al. (2012) and Diebold and Yilmaz (2014) show that the strength of connectedness of financial institutions changed over time, substantially increasing across market turmoils. In the spirit of Diebold and Yilmaz (2014), we provide a unifying framework to empirically measure systemic risk via direct inference on unobservable, time-varying, cross-firm linkages.

We take steps from this literature in several important directions. We propose a joint inference scheme on both the network structure and the model parameters in a single step. Standard empirical methodologies are based on pairwise correlation and Granger causality to build the economic network; these measures tend to overestimate the number of linkages, are static in nature and tied to linear Gaussian settings, which makes them of limited value for systemic risk measurement in dynamic contexts (see e.g. Forbes and Rigobon 2000, Ahelegbey, Billio, and Casarin 2014, and Diebold and Yilmaz 2014). In this paper, we propose a system-wide inference scheme based on an underlying undirected Graphical model, that allows to simultaneously consider all of the possible linkages among institutions in a large dimensional dynamic setting via parametric and conditional independence constraints.[2]

Also, we fully acknowledge the fact that parameters are uncertain. Existing methodologies extract the network structure assuming the parameters of the model are constant in repeated samples. As a result, the derived inference is thus to be read as contingent on the econometrician having full confidence in his parameters estimates. Yet, alternative conceivable values of the parameters will typically lead to different networks. In this paper, we provide a robust finite-sample Bayesian estimation framework which helps generate posterior distribution of virtually any function of the model parameters, as well as sufficient statistics for the underlying economic network. Such posterior estimates allow to test hypothesis on the nature and structure of the network linkages in a unified setting, which the earlier literature did not provide. Following

[2]See Whittaker (1990); Dawid and Lauritzen (1993), Lauritzen (1996), Carvalho and West (2007), Wang and West (2009) and Wang (2010) for more detailed discussions on graphical models and their applications.

previous research, we take into account the fact that contagion and systemic risk are more shift concepts than steady states (e.g. Forbes and Rigobon 2000, Billio et al. 2012 and Diebold and Yilmaz 2014). Based on this intuition we suggest the presence of distinct unobserved regimes driving the dynamics of network connectivity. Regimes are identified on the basis of a weighted eigenvector centrality measure, which allows to effectively separate states according to the density of the network.

Empirically, the paper focuses on a set of 100 blue-chip companies from the S&P100 Index. We consider those institutions with more than 15 years of historical data. We are left with 83 firms. Returns are computed on a daily basis, dollar-valued and taken in excess of the risk-free rate. The sample is 10/05/1996-31/10/2014 (4821 observations for each institution), for a total of more than 400,000 firm-day observations. Our emphasis on stock returns is motivated by the desire to incorporate the most current information for systemic risk measurement; stocks returns reflect information more rapidly than non-trading-based measures such as accounting variables, deposits, credits and loans, especially considering such information is mostly not available on a daily frequency.

We also consider the impact of common sources of systematic risk such as, for instance, the return of aggregate financial wealth in excess of the T-Bill rate, i.e. the CAPM. Specifying a factor model does not imply that we take a stand on the mechanism that transfers fundamentals shocks into cross-sectional dependence. Of course, given its residual nature, any statements on systemic risk will be conditional on a correct specification of the factor model (see, e.g. Bekaert et al. 2014). Our methodology is rather general and can be applied to any linear factor pricing model. To mitigate the model selection bias we consider other popular theory-based factor pricing models. In addition to the CAPM, we consider the three-factor model proposed by Fama and French (1993), and an implementation of the Merton (1973) intertemporal extension of the CAPM (I-CAPM) including shocks to aggregate dividend yield and both default- and term-spreads as state variables, in addition to aggregate wealth (see Petkova 2006). The results are robust across different factor model specifications. Data are from the Center for Research in Security Prices (CRSP), the FredII database of the St. Louis Federal Reserve Bank, Ibbotson Associates, and Kenneth French's website.

Our empirical findings show that we can identify two regimes of network connectivity, with high systemic risk characterizing financial markets across the period 1999/2003 (e.g. Gramm-Leach-Bliley act, dot.com bubble, Financial scandals), and the great financial crisis of 2008/2009. Few financial firms such as JP Morgan, Bank of America and Bank of New York Mellon turn out to play a key role for systemic risk management, as they heavily outweigh other firms within the economic network. This pattern holds also at the industry level, with industries classified according to the Global Industry Classification Standard (GICS) developed by MSCI. In fact, while the Energy sector is key within periods of low systemic risk, the financial sector is central for the propagation of firm-specific shocks when the economic network is dense. This evidence is in line with Barigozzi and Brownlees (2014) and Diebold and Yilmaz (2014).

Also, a simple cross-sectional regression analysis and rank-correlation coefficients show that firms that are central in the economic network do not have the highest average market value. We provide evidence that companies with higher network centrality, are more likely to suffer significant average maximum percentage losses when aggregate connectivity is bigger. In this respect, our network centrality measure is similar to the marginal expected shortfall (MES) originally proposed by Acharya et al. (2011), which tracks the sensitivity of firm ith's return to a systemic extreme event, thereby providing a market-based measure of firms fragility.

Finally, we show that both unexplained returns and exposures to sources of systematic risks changes across different regimes of aggregate network connectivity. For instance, the Jensen's alpha on financial firms tend to be lower when aggregate systemic risk is high, which corresponds to an increase in the exposures to market risk. By using a Probit regression analysis we show that our model-implied aggregate systemic risk measure is positively correlated with the business cycle.

The remainder of the paper proceeds as follows. Section 2 introduces Graphical models. Section 3 lays out our modeling setting. Section 4 discusses the data, the prior elicitation and reports the main empirical results. The relationship between systemic risk and value losses is investigated in Section 5. Section 6 investigates how network centrality relates to proxies for the business cycle. Section 7 concludes. We leave to the Appendix derivations details, results on a simulated dataset, and a set of convergence diagnostics.

2 Background on Gaussian Graphical Models

Graphical models are statistical objects that summarize the marginal and conditional independences within a set of random variables by means of graphs. A graph is characterized by the pair $G_t = (V, E_t)$ where V is the vertex set of N nodes and E_t defines the edge-set, where the nodes represent the variables of the system and the edges define the nature of the interconnections. Let $X_t = (X_{1,t}, \cdots, X_{N,t}) \in \mathbb{R}^N \sim N(0, \Sigma_t)$, where $X_{i,t}$ is the realization of the ith variable at time t. If the vertices V of this graph are put in correspondence of each firm, the edge set E_t induces conditional independence relationships on X_t via a Markov property of the nodes (see Erdös and Rényi 1959, Dempster 1972, Dawid and Lauritzen 1993, Giudici and Green 1999 and Carvalho and West 2007 for more details).

More precisely, the Markov property determined by G_t states that, for all $1 \leq i < j \leq N$,

$$e_{ij,t} = 0 \Leftrightarrow X_{i,t} \perp X_{j,t} | X_{V \setminus \{i,j\}}$$

Therefore, the correlation between $X_{i,t}$ and $X_{j,t}$ conditionally on the remaining variables $X_{V \setminus \{i,j\}}$ is null as far as the structure implied by the graph $G_t = (V, E_t)$ constrain an edge to be equal to zero. Figure 1 shows an example of an undirected graph in which $V = \{1, 2, 3, 4, 5, 6, 7, 8\}$, and linkages are represented by covariance terms $E_t = \{\sigma_{12}, \sigma_{13}, \sigma_{23}, \sigma_{45}, \sigma_{46}, \sigma_{56}, \sigma_{78}\}$.

[Insert Figure 1 about here]

Such sparse structure allows to decompose the conditional covariance structure of X_t reducing a high-dimensional problem to a collection of local linkages. Using the framework of Dawid and Lauritzen (1993), Giudici and Green (1999) and Carvalho and West (2007), we can define Σ_t as an *Hyper-Inverse Wishart* (HIW) distribution, with *hyper-parameters* (d, D) denoted by $\Sigma_t | G_t, d, D \sim HIW(G_t, d, D)$, if for $\Sigma_t \in \mathcal{M}(G_t)$ the set of all positive-definite symmetric matrices with elements equal to zero for all $(i, j) \notin E_t$;

$$p(\Sigma_t | G_t, d, D) = \frac{\prod_{c \in \mathcal{C}} p(\Sigma_t^c | d^c, D^c)}{\prod_{s \in \mathcal{S}} p(\Sigma_t^s | d^s, D^s)}, \tag{1}$$

where for each $c \in \mathcal{C}$, $\Sigma_t^c \sim IW\left(d^c, D^c\right)$ and $s \in \mathcal{S}$, $\Sigma_t^s \sim IW\left(d^s, D^s\right)$ (see Hammersley and Clifford 1971 and Dempster 1972).

3 A Markov Regime-Switching Factor Pricing Approach

We assume systematic risk factors are common across institutions, and consider a seemingly unrelated regression (SUR) model. Let y_{it} represents the *excess* returns on the ith institution at time t, and $\mathbf{x}_{it}$ the n_i-dimensional vector of systematic risk factors with possibly a constant term for individual i at time t; the model dynamics can be summarized as

$$\mathbf{y}_t = X_t' \tilde{\boldsymbol{\beta}}_t + \boldsymbol{\varepsilon}_t, \qquad \boldsymbol{\varepsilon}_t \sim \mathcal{N}_N\left(\mathbf{0}, \tilde{\Sigma}_t\right) \tag{2}$$

$t = 1, \ldots, T$, where $\mathbf{y}_t = (y_{1t}, \ldots, y_{Nt})'$ is a N-dimensional vector of returns in excess of the risk-free rate, $X_t = \text{diag}\{(\mathbf{x}_{1t}', \ldots, \mathbf{x}_{Nt}')\}$ a $p \times N$ matrix of explanatory variables plus intercept, with $p = \sum_{i=1}^{N} n_i$, $\boldsymbol{\varepsilon}_t = (\varepsilon_{1t}, \ldots, \varepsilon_{Nt})'$ the vector of normal random errors, and $\tilde{\boldsymbol{\beta}}_t = \left(\tilde{\beta}_{1t}, \ldots, \tilde{\beta}_{Nt}\right)'$ the $p-$dimensional vector of betas at time t. The dynamics described in (2) is fairly general since represents an approximation of a reduced-form stochastic discount factor where the risk factors are assumed to capture business cycle effects on investors' beliefs and/or preferences (see Liew and Vassalou 2000, Cochrane 2001, and Vassalou 2003).

The variance-covariance matrix $\tilde{\Sigma}_t$ is consistent with the restrictions implied by the underlying undirected graph G_t, and thus reflects the level of network connectivity at time t.[3] We assume that the vector of exposures to systematic risks $\tilde{\boldsymbol{\beta}}_t$, the covariance matrix $\tilde{\Sigma}_t$, and the network G_t have a Markov regime-switching dynamics. They are driven by an unobservable state $s_t \in \{1, \ldots, K\}$, $t = 1, \ldots, T$, that takes a finite number K of values and represents network system-wide connectedness, namely systemic risk. Such state s_t evolves as a Markov chain process, where the transition probability π_{ij}, of going from the ith to the jth state in one step is time-invariant (see, e.g. Hamilton 1994), that is $P(s_t = i | s_{t-1} = j) = \pi_{ij}$, $i, j = 1, \ldots, K$, for all $t = 1, \ldots, T$.

[3] Given the residual nature of systemic risk with respect to sources of systematic risk, we assume the graph is undirected, meaning there is no particular direction in the conditional dependence structure among firms. However, directed graphical models can be also accomplished within our modeling framework and we leave that for future research.

The choice of a Markov regime-switching dynamics is motivated by the common definition of contagion and systemic risk as abrupt increases in the cross-sectional dependence structure of institutions/sectors/countries after a shock (see e.g. Forbes and Rigobon 2000). Also, the Markov regime-switching nature of the covariance structure allows to acknowledge the heteroskedasticity bias highlighted in Forbes and Rigobon (2002).[4] As typical in SUR models we assume that the exogenous shocks are possibly contemporaneously correlated, but not autocorrelated, i.e. we assume the graph structure G_t is undirected. The Markov-switching graphical model specification in equation (2) makes the exposures to sources of systematic risk time varying and directly depending on the regime of systemic risk;

$$\tilde{\boldsymbol{\beta}}_t = \sum_{k=1}^{K} \boldsymbol{\beta}_k \mathbb{I}_{\{k\}}(s_t) \tag{3}$$

with $\mathbb{I}_{\{k\}}(s_t)$ the indicator function which takes value one when the state s_t takes value k at time t and zero otherwise. The state-specific covariance matrix Σ_k is constrained by a sate-specific graph G_k, that is

$$\tilde{\Sigma}_t = \sum_{k=1}^{K} \Sigma_k(G_k)\, \mathbb{I}_{\{k\}}(s_t), \qquad \tilde{G}_t = \sum_{k=1}^{K} G_k \mathbb{I}_{\{k\}}(s_t) \tag{4}$$

with $\Sigma_k \in \mathcal{M}(G_k)$ and $\mathcal{M}(G_k)$ the set of all positive-definite symmetric matrices with elements equal to zero for all $(i,j) \notin E$, given the state $s_t = k$. In the model, contagion is generated by both the number of edges in $\tilde{G}_t$ when $s_t = k$, and the magnitude of the dependence between nodes measured by the covariance terms. Traditional connectedness measures do not distinguish between these two sources and therefore may result in biased estimates. Also, the features of the state-specific graph G_k play a crucial role in the estimation of our regime-switching model, since they allow us to identify the regimes of low and high systemic risk exposure.

[4] Markov regime-switching models are popular in the finance literature since Ang and Bekaert (2002), Guidolin and Timmermann (2007), and Guidolin and Timmermann (2008), as they allows for both statistical identification and economic interpretation of different market phases.

3.1 Network Connectivity Measures

In this paper, we assume that a connectivity measure $q = h(G_k)$ is a map function h from the graph space $\mathcal{G}$ to the set of the real numbers $Q \subset \mathbb{R}$. These measures can be used to measure risk relying on the network structure and to identify systemic risk regimes. Different concentration measures have been proposed in the literature. These include average degree, closeness, betweenness, and eigenvector centrality. To use the correct measure for systemic risk purposes, we must first consider the consistency of the assumptions underlie each measure with the concept of systemic risk. Although making generalization of the propagation mechanism of exogenous shocks is problematic, one can make few reasonable assumptions about how shocks can flow from one firm to another within the economic system.

First, regardless of the inherent definition of an economic shock, they are unlikely to follow the shortest path between two nodes. Only shocks with known destination follow the shortest possible distance (e.g. tag a recipient with twitter). Economic shocks are unlikely to be restricted to follow specific paths but likely have feedback effects. For instance, a liquidity shock on a single firm could affect the ability to repay a loan to a bank, that could prevent the bank to allow for credit line to another firm, that in turns can no longer afford to pay for supply debits, which eventually could flaw back to the original firm if there is a trade relationship. According to Borgatti (2005), this means that closeness and betweenness centrality are inappropriate for economic shocks since they implicitly assume a pre-determined path.

Second, linkages among firms are not all equal. Firms in large sectors such as "industrials" are likely highly connected to other firms through supply relationships. This implies that the average number of linkages of the industrial sector could be high by definition. However, this does not imply that a demand shock to Fedex is necessarily more systemical important than a liquidity shock to JP Morgan. This rules out average degree centrality. Indeed, such measure gives a simple count of the number of connections a company has, without effectively discriminating the relative importance of these connections with respect to the whole network.

Based on this, we propose a weighted centrality measure based on the adjacency matrix A_t explained above, where the weights are defined by the covariance terms. Eigenvector centrality is closely related to "PageRank" used in web search engines and acknowledges the fact that cross-

firms connections are not all equal, considering the actual influence of a company in the economic network. By weighing for the covariance terms we can compute the marginal contribution of a single firm to aggregate systemic risk as a function of the quality of its connections with other firms, and the magnitude of the linkages expressed by the covariance terms. For the *ith* firm, weighted eigenvector centrality is defined to be proportional to the sum of centralities of the vertex's neighbours, so that the firm can acquire higher centrality by being connected to a lot of other firms or by being connected to others that themselves are highly central;

$$x_{i,k} = \frac{1}{\lambda_k} \sum_{j=1}^{n} a_{ij,k} x_{j,k} = \frac{1}{\lambda_k} \sum_{j \in N(i,k)} \sigma_{ij,k} x_{j,k} \tag{5}$$

where $N(i,k) \subset V$ the set of neighbours of i given the state $s_t = k$, that is $N(i,k) = \{j \in V : a_{ijk} = 1\}$. Equation (5) can be rewritten in a more compact form as $A_k x_k = \lambda_k x_k$, such that $q_{E,k} = x_{j^*,k}$, with A_k the adjacency matrix in which each entry denoted $a_{ij,k}$, for row i column j and state k, records the existence and strength of linkages between the institution i and j[5];

$$a_{ij,k} = \begin{cases} \sigma_{ij,k} & \text{if } i \text{ and } j \text{ are connected in state } k \\ 0 & \text{otherwise} \end{cases} \tag{6}$$

with $x = (x_1, x_2, \ldots, x_p)$, and $j^* = \arg\max\{\lambda_j, j = 1, \ldots, n\}$ is the index corresponding to the greatest Laplacian eigenvalue, λ_j, $j = 1, \ldots, n$, are the Laplacian eigenvalues.[6] For this measure $Q = \mathbb{R}$ with larger values indicating higher centrality. Firm-specific eigenvector centrality can be generalized at the industry level by averaging $x_{i,k}$ within a certain industry. For instance, the weighted eigenvector centrality for the financial sector can be approximated as

$$x_{f,k} = \frac{1}{n_f} \sum_{i \in V_f} x_{i,k} \tag{7}$$

with $n_f = |V_f|$, and $V_f \subset V$ the set of nodes associated to firms classified as "financials" according to the GICS. If the adjacency matrix has non-negative entries, a unique solution is guaranteed to exist by the Perron-Frobenius theorem. Our weighted eigenvector centrality is

[5]Intuitively, A_s allows to compute firm-specific systemic risk contributions based on direct connections a firm has and to which other firms these connections are made.

[6]The Laplacian eigenvalues are the eigenvalues arranged in non-increasing order of the Laplacian matrix, $L = D - A$, where $D = \text{diag}\{d_1, \ldots, d_n\}$ is a diagonal matrix with the vertex degree on the main diagonal. Here, $\mathbf{z}_j$, $j = 1, \ldots, n$, are the corresponding Laplacian eigenvectors.

also related to a standard principal component analysis (PCA) (see e.g. Billio et al. 2012). Just as PCA analysis our measure identify the concentration of the economic system weighing for the cross-sectional variance-covariance matrix of the firms. To summarize, (5) measures not only the likelihood that an exogenous shock transmits to the ith firm, but also the magnitude of the effect of the shock on itself. For the sake of completeness, in the following we also report the results based on a standard eigenvector centrality measure which does not weight for the covariance terms.

3.2 Inference on Networks and Parameters

Our estimation approach generalizes earlier literature and consider a joint inference scheme on networks, covariances and factor model parameters in a large dimensional time series setting. Given the fairly relevant complexity and non-linearity of the model, we opted for a Bayesian estimation scheme of the network G_k and the structural parameters $\boldsymbol{\theta}_k = (\boldsymbol{\beta}_k, \Sigma_k, \boldsymbol{\pi}_k)$, with $\boldsymbol{\pi}_k$ the kth row of the transition matrix Π for the latent state, $s_t = k$. Also, by using Bayesian tools we can generate posterior distributions of virtually any sufficient statistics for the underlying network, as well as for any of the structural parameters of the linear factor pricing model.

3.3 Prior Specification

For the Bayesian inference to work, we need to specify the prior distributions for the network and the structural parameters. For a given graph G_k and state $s_t = k$ the prior structure is conjugate and the model dynamics (2) reduces to a standard SUR model (e.g., see Chib and Greenberg 1995). This makes Bayesian updating straightforward and numerically feasible. As far as the systemic risk state transition probabilities are concerned we choose a Dirichlet distribution:

$$(\pi_{k1}, \ldots, \pi_{kK}) \sim \mathcal{D}ir\,(\delta_{k1}, \ldots, \delta_{kL}) \tag{8}$$

with δ_{ki} the concentration parameter for π_{ki}, and $\Pi_k = (\pi_{k1}, ..., \pi_{kK})$ the kth row of the transition matrix Π. The role of the covariance structure Σ_k is one of the most important in the SUR model specification. The non-diagonal structure of the residual covariance matrix

improves parameter estimation by exploiting shared features of the $p-$dimensional vector of excess returns. However, an increasing p makes complexity unfeasible to be managed. In this context we take advantage of natural restrictions induced by the network structure (Carvalho and West 2007,Carvalho, West, and Massam 2007, and Wang and West 2009).

The prior over the graph structure is defined as a Bernoulli distribution with parameter ψ on each edge inclusion probability as an initial sparse inducing prior. That is, a p node graph $G_k = (V_k, E_k)$ with $|E_k|$ edges has a prior probability

$$\begin{aligned} p(G_k) &\propto \prod_{i,j} \psi^{e_{ij}} (1-\psi)^{(1-e_{ij})} \\ &= \psi^{|E_k|} (1-\psi)^{T-|E_k|} \end{aligned} \tag{9}$$

with $e_{ij} = 1$ if $(i,j) \in E_k$. This prior has its peak at $T\psi$ hedges, with $T = p(p-1)/2$, for an unrestricted p node graph, providing a flexible way to directly control for the prior model complexity. A uniform prior alternative might be used. However as pointed out in Jones, Carvalho, Dobra, Hans, Carter, and West (2005), a uniform prior over the space of all graphs is biased towards a graph with half of the total number of possible edges. As the number of possible graphs for a p node structure is, for large p, the uniform prior gives priority to those models where the number of edges is quite large. To induce sparsity and hence obtain a parsimonious representation of the interdependence structure implied by a graph, we choose $\psi = 2/(p-1)$ which would provide a prior mode at p edges.

Conditional on a specified graph G_k and state $s_t = k$, the hyper inverse-Wishart is denoted as

$$\Sigma_k \sim \mathcal{HIW}_{G_k} (d_k, D_k) \tag{10}$$

with d_k and D_k respectively the degrees of freedom and the scale hyper-parameters. This distribution is the unique conjugate "local prior" for any covariance $\Sigma_t (G_t)$ with marginals for the cliques which are inverse Wishart distributed (see Appendix A). The prior for the betas is

independent on the covariance structure,

$$\boldsymbol{\beta}_k \sim \mathcal{N}_p\left(\mathbf{m}_k, M_k\right) \tag{11}$$

with $\mathbf{m}_k$ and M_k the location and scale hyper-parameters, respectively.[7] The choice of the prior hyper-parameters is discussed in Section 4.

3.4 Posterior Approximation

In order to find a Bayesian estimation of the parameters, the graphs and the latent states we follow a data augmentation principle (see Tanner and Wong 1987) which relies on the complete likelihood function, that is the product of the data and state variable densities, given the parameters and the graphs. Let us denote with $\mathbf{z}_{s:t} = (\mathbf{z}_s, \ldots, \mathbf{z}_t)$, $s \leq t$, a collection of vectors $\mathbf{z}_u$. The collections of graphs and parameters are defined as $G = (G_1, \ldots, G_K)$ and $\boldsymbol{\theta} = (\boldsymbol{\theta}_1, \ldots, \boldsymbol{\theta}_K)$, respectively, where $\boldsymbol{\theta}_k = (\boldsymbol{\beta}_k, \Sigma_k, \boldsymbol{\pi}_k)$, $k = 1, \ldots, K$, are the state-specific parameters. The completed data likelihood is

$$p\left(\mathbf{y}_{1:T}, \mathbf{s}_{1:T} | \boldsymbol{\theta}, G\right) = \prod_{k,l=1}^{K} \prod_{t=1}^{T} (2\pi)^{-n/2} \left|\tilde{\Sigma}_t\right|^{-n/2} \exp\left(-\frac{1}{2}\left(y_t - X_t'\tilde{\boldsymbol{\beta}}_t\right)' \tilde{\Sigma}_t^{-1}\left(y_t - X_t'\tilde{\boldsymbol{\beta}}_t\right)\right) p_{kl}^{N_{kl,t}} \tag{12}$$

with $N_{kl,t} = \mathbb{I}_{\{k\}}\left(s_{t-1}\right)\mathbb{I}_{\{l\}}\left(s_t\right)$. Combining the prior specifications (8)-(11) with the complete likelihood (12), we obtain the posterior density

$$p\left(\boldsymbol{\theta}, G, \mathbf{s}_{1:T} | \mathbf{y}_{1:T}\right) \propto p\left(\mathbf{y}_{1:T}, \mathbf{s}_{1:T} | \boldsymbol{\theta}, G\right) p(\boldsymbol{\theta}, G) \tag{13}$$

Since the joint posterior distribution is not tractable the Bayesian estimator of the parameters and graphs cannot be obtained in analytical form, thus we approximate the posterior distribution and the Bayes estimator by simulation. The random draws from the joint posterior distributions are obtained through a Gibbs sampler algorithm (Geman and Geman 1984). We propose a collapsed multi-move Gibbs sampling algorithm (see e.g. Roberts and Sahu 1997

[7] Notice that the fact that priors for the covariance structure and the betas are independent does not mean they are sample independently in the Gibbs sampler. Indeed, in the sampling scheme they are sampled conditionally on each other iteratively, and therefore can be thought as coming from the same joint distribution asymptotically.

and Casella and Robert 2004), where the graph structure, the hidden states and the parameter are sampled in blocks. More specifically we combine forward filtering backward sampling (see Frühwirth-Schnatter 1994 and Carter and Kohn 1994 for more details) for the hidden states, an efficient sampling algorithm for the covariance structure (see Carvalho and West 2007, Carvalho et al. 2007 and Wang and West 2009), and multi-move MCMC search for graph sampling (see e.g. Giudici and Green 1999 and Jones et al. 2005). At each iteration the Gibbs sampler sequentially cycles through the following steps:

1. Draw $\mathbf{s}_{1:T}$ conditional on $\boldsymbol{\theta}$, G and $\mathbf{y}_{1:T}$.
2. Draw Σ_k conditional on $\mathbf{y}_{1:T}$, $\mathbf{s}_{1:T}$, G_k and $\boldsymbol{\beta}_k$.
3. Draw G_k conditional on $\mathbf{y}_{1:T}$, $\mathbf{s}_{1:T}$ and $\boldsymbol{\beta}_k$.
4. Draw $\boldsymbol{\beta}_k$ conditional on $\mathbf{y}_{1:T}$, $\mathbf{s}_{1:T}$ and Σ_k.
5. Draw $\boldsymbol{\pi}_k$ conditional on $\mathbf{y}_{1:T}$, $\mathbf{s}_{1:T}$.

From step 2 to 3 the Gibbs sampler is collapsed as G_k is drawn without conditioning on Σ_k since they are conditionally independent. In fact, the graph G_k is sampled marginalizing over the covariance structure Σ_k (see Carvalho and West 2007, Carvalho et al. 2007 and Wang and West 2009). A detailed description of the Gibbs sampler is given in the Appendix.

Inference on Markov-switching models, requires dealing with the identification issue arising from the invariance of the likelihood function to permutations of the hidden state variables. Different solutions to this problem have been proposed in the literature (see Frühwirth-Schnatter 2006 for a review). In this paper, we contribute to this stream of literature providing a way to identify regimes through graphs. More specifically we suggest to identify the regimes by imposing the following constraints on the state-specific graphs. We consider the following identification constraints $q(G_1) < \ldots < q(G_K)$, where q is the average weighted eigenvector centrality, i.e. $\frac{1}{N}\sum_{i=1}^{N}\tilde{x}_{i,k}$ for $k = 1, ..., K$. This constraint allows us to interpret the first regime as the one associated with the lowest systemic risk level and the last regime as the one associated with the highest risk. In context where the eigenvector centrality is not sufficient to achieve a characterization of the regimes, then a complexity measure (see, e.g. Newman 2003, Emmert-Streib and Dehemer 2012), which combines information from different network measures, can be employed. From a practical point of view, we find in our empirical applications

that eigenvector centrality ordering works as well as degree centrality constraint for the regime identification.

Given the prior distribution assumption and the Graphical model defined above, it is possible to define a posterior distribution of the graph $p(G_k|\mathbf{y}_{1:T})$ and to assess the statistical properties of the network measures by employing the distribution defined by the transform $q = h(G_k)$. We develop a Gibbs sampling to generate samples from the graph posterior distribution, which can be used to approximate also the connectedness measure distribution;

$$p_J(q_k|\mathbf{y}_{1:T}) = \frac{1}{J}\sum_{j=1}^{J}\delta_{q_k^j}(q_k) \tag{14}$$

where $q_k^j = h(G_k^{(j)})$ and $G_k^{(j)}$ is the jth sample from the graph posterior distribution for the state $s_t = k$, and J is the number of Gibbs iterations. Usually, once a graph is estimated the network measure is applied to this graph, thus all information about graph uncertainty are lost. In this paper we propose to account for the uncertainty associated with the graph G_k, and suggest the following integrated measure and its MCMC approximation

$$\int_{\mathcal{G}_k} h(G_k)p(G_k|\mathbf{y}_{1:T})dG_k \approx \int_Q q_k\, p_J(q_k|\mathbf{y}_{1:T})dq_k$$

which is the empirical average of the sequence of measures q_k^j, $j = 1, \ldots, J$, associated with the MCMC graph sequence. As a whole, from the Bayesian scheme we can make robust hypothesis testing on the network structure as we are able to approximate, at least numerically, the entire distribution of networks conditioning on the state of contagion.

4 Empirical Analysis

As empirical application we measure systemic risk for a large set of companies. Systemic risk is jointly considered with sources of systematic risk which are assumed to capture investors' beliefs on the business cycle (see Liew and Vassalou 2000, Cochrane 2001, Vassalou 2003, and Campbell and Diebold 2009). In particular, while the exposure to sources of systematic risk (i.e. betas) depends on the state of systemic risk, the latter directly depends on the betas given

its residual nature. As such, although conditionally independent, systematic and systemic risks are not mutually exclusive. In order to mitigate the selection bias for systematic risk factors we considered alternative theory-based leading factor pricing model specifications. However, our methodology is rather general and can be easily applied to any linear factor pricing model.

4.1 Data and Factor Pricing Models

We focus on the 100 blue chip companies that compose the S&P100 Index. We consider those institutions with more than 15 years of historical available data at the daily frequency, for a total of 83 companies. Table 1 summarize the firms in our dataset and the corresponding industry classification according to the Global Industry Classification Standard (GICS), developed by MSCI. Returns are dollar-valued and computed daily in excess of the risk-free rate. The sample period is 05/10/1996-10/31/2014, for a total of more than 400,000 firm-day observations. Our emphasis on stock returns is motivated by the desire to incorporate the most current information in the network analysis; stocks returns reflect information more rapidly than non-trading-based measures such as accounting variables.

[Insert Table 1 about here]

We analyse three representative asset pricing models starting from the simple CAPM, which implies a unique risk factor represented by the excess return (in excess of the 1-month T-Bill rate) on the aggregate value-weighted NYSE/AMEX/NASDAQ index, taken from the Center for Research in Security Prices (CRSP). The return on the 1-month T-Bill rate is taken from Ibbotson Associates.

The second model considered is the well-known three-factor model initially proposed in Fama and French (1993). This model includes two empirically motivated risk factors in addition to the simple CAPM; the return spread between portfolios of stocks with small and large market capitalization, i.e. *SMB*, and the return difference between "value" and "growth" stocks, namely portfolios of stocks with high and low book-to-market ratios, i.e. *HML*.

Next, we consider an implementation of the Merton (1973) intertemporal CAPM. Based on Campbell (1996), who argues that innovations in state variables that forecasts changes in

investment opportunities should serve as risk factors, we use aggregate dividend yield and both default- and term-spreads as state variables, in addition to aggregate wealth (see Petkova 2006 for an example). Default spread is computed as the difference between the yields of long-term corporate Baa bonds and long-term government bonds. The term spread is measured the difference between the yields of 10- and 1-year government bonds. Data on bonds and treasuries are taken from the FredII database of the Federal Reserve Bank of St.Louis.

We adopt the approach of Campbell (1996) and compute the changes in risk factors as the innovations of a first order Vector Auto-Regressive (VAR(1)) process. Thus, for each collection of the CRSP aggregate value-weighted market portfolio and the candidate set of risk factors $h_t = (r_{m,t}, \quad x_t')'$, we estimate $h_t = B_0 + B_1 h_{t-1} + e_t$ for $t = 1, \ldots, T$. Following Petkova (2006), the innovations e_t are orthogonalized from the excess return on the aggregate wealth and scaled to have the same variance.

4.2 Prior Choices and Parameters Estimates

Realistic values for different prior distributions obviously depend on the problem at hand. For the transition mechanism of systemic risk the prior hyper-parameters of the Dirichlet distribution are taken such that a priori systemic risk is persistent. Such prior belief is mainly based on the common wisdom that increasing network connectedness is not a quickly mean-reverting process (see e.g. Forbes and Rigobon 2002).

Given the large dimensional setting of the model, training the priors with firm-specific information is prohibitive. We take an agnostic perspective in setting the hyper-parameters of the betas across institutions. The prior location parameter $m_k = 0$ for each $k = 1, ..., K$. The corresponding prior scale is set equal to $M_k = 1000 I_p$ across states. Notice we do not force posterior estimates in any direction across states as the prior structure does not differ across low vs high systemic risk states.

The prior degrees of freedom and scale of the Hyper-Inverse Wishart distribution for the conditional covariance matrix are set to be $d_k = 3$ and $D_k = 0.0001 I_p$, respectively. This is also a fairly vague, albeit proper, prior distribution. Finally, the prior for the graph space is a Bernoulli distribution. We have chosen an hyper-parameter equal to $\psi = 2/(p-1)$ which

would provide a prior mode at p edges. We could alternatively use a uniform prior over the space of all graphs. However as pointed out in Jones et al. (2005), a uniform prior would be biased towards a graph with half of the total number of possible edges. For large p, the uniform prior gives priority to those models where the number of edges is quite large.

In order to further reduce the sensitivity of posterior estimates to the prior specification, we use a burn-in sample of 2,000 draws storing every other of the draws from the residuals 10,000 draws (see e.g. Primiceri 2005). The resulting auto-correlations of the draws are very low. A convergence analysis in Appendix C shows that this guarantees accurate inference in our network based linear factor model.

Figure 2 shows the systemic risk probability over the testing sample, computed from the CAPM (top-left panel), the Fama-French three-factor model (bottom-left panel) and the I-CAPM implementation with default-, term-spread and the aggregate dividend yield in addition to aggregate wealth as risk factors (top-right panel). The gray area represents the systemic risk probability, while the blue line shows the NBER recession indicator for the period following the peak of the recession to the through.

[Insert Figure 2 about here]

The figure makes clear that high systemic risk characterized the period 2001/2002 (i.e. dot.com bubble, 9/11 attacks, Financial scandals, Iraq war), and the great financial crisis of 2008/2009. Although there is mis-matching with respect to the business cycle indicator across the period 1998-2002, the NBER recession and high systemic risk tend to overlap across the recent great financial crisis.

Bottom-right panel shows the transition probabilities across models. The first (last) three columns represent the probability of staying in a state of low (high) systemic risk. Systemic risk persists with an average probability of $\pi_{hh} = 0.93$, implying that the duration of a period of high systemic risk is around $1/(1-\pi_{hh}) = 14$ days, while the long run probability of high systemic risk is equal to $(1-\pi_{ll})/(2-\pi_{hh}-\pi_{ll}) = 0.33$. This means that, in our sample tend the economy tend to be affected by high systemic risk for about a third of trading days, unconditionally. Figure 3 shows changes in abnormal returns and exposures to sources of systematic

risks from low to high systemic risk, computed from the Fama-French three-factor model. For the sake of exposition, results are labeled according to the GISC industry classification. Top left panel shows the difference in the intercepts across companies. The figure makes clear that the Jensen's alphas do not change across different regimes of systemic risk in a significant way. Indeed, the zero line never falls outside the 95% confidence interval of the model estimates. Interestingly, the differences in exposures to the aggregate wealth risk factor is significantly negative for financial firms. This implies that the exposure to market risk of financial firms increases when systemic risk is higher. The only exception within the financial sector is the Berkshire Hathaway Inc. of Warren Buffett.

[Insert Figure 3 about here]

Similarly, financial firms are more exposed to value risk when systemic risk is higher. Two exceptions are again Berkshire Hathaway Inc., together with Morgan Stanley. Also Citigroup, although has negative difference on the HML beta, it is not statistically significant. The Industrial and Materials sectors also show an increasing exposure to value premium when systemic risk is higher. Figure 4 shows changes to the conditional betas on shocks to macroeconomic risk factors in the I-CAPM implementation. As we would expect, the behavior of the betas on market risk is consistent with the Fama-French three-factor model. The only exception is again Berkshire Hathaway Inc., although the difference in the beta is negative, on average.

[Insert Figure 4 about here]

Interestingly, the Energy sector shows the opposite path with respect to Financials. In fact, the exposure to market risk of energy stocks tend to be lower when systemic risk is higher. Bottom left panel shows the change of exposures to default risk from low vs. high systemic risk. On average, exposure to default risk is higher when systemic risk is higher, although for a large fraction of the sample such negative delta is not statistically significant. In the financial sector, AIG, Morgan Stanley, Bank of America, and American Express tend to be more exposed to default risk when systemic risk increases. In the technology sector Microsoft, IBM, Intel and Oracle are more exposed to default risk during market turmoils. Bottom right panel shows that

Energy and Financials are less exposed to the aggregate dividend yield when systemic risk is high.

4.3 Financial Networks

Thus far we have introduced tools to measure systemic risk. We now put those tools at work and investigate the evolution of networks connectedness over time. Figure 5 shows the connectivity of firms inferred from the residuals of the CAPM. The size and the color of the nodes are proportional to their relevance in the network measured by weighted eigenvector centrality (5). The darker (bigger) the color (size) of the node, the higher its marginal contribution to aggregate systemic risk.

[Insert Figure 5 about here]

Left panel shows the network in regime one. Figure 5 makes clear that Energy companies such as ConocoPhillips (COP), Apache (APA), Occidental Ptl. (OXY), Exxon (XOM) and Schlumberger (SLB) are central for the economic system when the aggregate systemic risk is low. Interestingly, few consumer companies such as Wal Mart (WMT), Costco (COST), Target (TGT), and Lowe's (LOW) are tightly link to each other, although completely disconnected from the rest of the economy. The financial sector turns out to be less relevant than the energy sector. Financial firms such as JP Morgan (JPM), AIG, Bank of America (BAC) and Wells Fargo (WFC), although present a significant weighted centrality, are not as relevant as, for instance, Exxon Mobil.

Right panel of Figure 5 shows how the network structure changes when aggregate systemic risk is high. The financial sector becomes a key factor in the transmission mechanism of exogenous shocks with firms such as JP Morgan and Citigroup playing a major role. Figure 2 and Figure 5 combined, confirm that during market turmoils, the systemic importance of the financial sector substantially increases. The marginal importance of each firm on the economic system as a whole might be uniquely driven by their relative market size, or valuation. Figure 6 address this issue by showing the network connectivity measured from residuals of a the three-factor Fama-French model which explicitly condition on size and book-to-market as aggregate

sources of systematic risks.

[Insert Figure 6 about here]

Left panel shows network connectivity when aggregate systemic risk is low. Figure 6 confirms the key role of the Energy sector. Exxon (XOM) and Schlumberger (SLB) carry a relevant fraction of systemic risk. Interestingly, by controlling for size and value, the role of the financial sector when systemic risk is low decreases relatively to other sectors such as Healthcare and Materials. Also, the economic network is now more sparse with lots of missing linkages. The energy and the financial sectors seem to create a sub-network themselves. Consistent with Figure 5, right panel of Figure 6 shows the key role of the financial sector in the network connectedness when aggregate systemic risk increases.

Finally, Figure 7 shows the network computed from the residuals of the I-CAPM implementation including default and interest rate risks, in addition to aggregate wealth and dividend yield. Left panel shows connectivity when aggregate systemic risk is low. The results confirm what shown above. The Energy sector turns out to be most systemically important sector. Interestingly, by conditioning on macroeconomic risk factors, Health Care becomes more important. Johnson & Johnson (JNJ) is as important as major firms of the Material sector. Abbot Labs (ABT), Eli Lilly (LLY), and Merck & Company (MKR), are as important as Bank of America (BAC), AIG, JP Morgan (JPM) and Wells Fargo (WFC) in terms of individual contribution to aggregate systemic risk.

[Insert Figure 7 about here]

As shown in Figure 5, few consumer discretionary and staples companies such as Wal Mart (WMT), Costco (COST), Target (TGT), Lowe's (LOW) and CVS are tightly link to each other, although disconnected from the rest of the economy. Similarly, Industrials such as 3M, United Tech (UTX), Boeing (BA), Honeywell Intl. (HON), Union Pacific (UNP), and Caterpillar (CAT) are disjoint from the rest of the economy although highly relevant in terms of aggregate systemic risk and connected to each other. Right panel shows the network connectedness when aggregate systemic risk is high. The Energy and Health Care sectors decrease their relevance. Financials such as Bank of America (BAC), AIG, JP Morgan (JPM), Wells Fargo (WFC),

Citigroup (C), and Bank of New York Mellon (BK) are now key for the transmission mechanism of individuals exogenous shocks to the whole economy. Consumer discretionary and staples are now connected to the rest of the economy through Procter & Gamble (PG). As a whole, Figures 5-7, together with Figure 2 make clear that Financials are systemically important when the network connectivity is high. As such, as an exogenous shocks on these institutions can quickly and heavily affect the entire economic system.

4.3.1 Firm-Level Network Centrality. We now focus our attention to the contribution of single firms to aggregate systemic risk. Figure 8 shows the top 20 institutions ranked according to their median weighted eigenvector centrality (5), which defines a measure of systemic importance of the single firm in the transmission mechanism of firm-specific exogenous shocks to the whole economic system. The median is computed across posterior simulations of the network structure as provided by equation (14). The red line (blue line) with circle (square) marks shows the centrality measure across companies when aggregate network connectedness is low (high).

[Insert Figure 8 about here]

Panel A shows the results conditioning on aggregate financial wealth as a unique source of systematic risk (i.e. CAPM). Energy companies such as Exxon Mobil (XOM) and Occidental Ptl. (OXY) show the highest weight under a regime of low network connectivity (red line, circle marks). Given the overall lower level of connectedness, the corresponding centrality measures are low in magnitude albeit significant. Financial firms such as Bank of New York (BK) and JP Morgan (JPM) rank 10th and 13th, respectively. The insurance sector giant AIG does not seem to be systemically important ranking 19th when systemic risk is low. Consistently with Figures 5-7 the systemic importance of Financials increases when network aggregate network connectivity increases. Now, JP Morgan (JPM) and Bank of New York (BK) turns out to be highly important for the economic system. Also, AIG now ranks 6th and carries a large weighted centrality for the economic network.

Panel B of Figure 8 shows the same weighted eigenvector centrality computed conditioning on size and value measured by book-to-market ratio, in addition to aggregate wealth. Energy stocks such as Exxon Mobil (XOM) shows a large weight when aggregate systemic risk is

relatively low. In the second state, Financials are again key for systemic risk management. Bank of America (BAC), for instance, is weighted more than the double of Exxon Mobil (XOM) and for times more than ConocoPhillips (COP). Also, Panel B shows that the network is much more concentrated around financial firms. This is consistent with the idea that systemic risk and systematic risks, although are not directly depending on each other, are not mutually exclusive. For instance, the average, median, eigenvector centrality under high systemic risk is around 0.017 with the three-factor Fama-French model, against the modest 0.009 obtained from the CAPM.

Bottom panel of Figure 8 shows median weighted eigenvector centrality computed from the I-CAPM implementation with shocks to macroeconomic risk factors. Interestingly, Johnson & Johnson carries the highest systemic risk. This is consistent with idea that by considering macroeconomic factors lowers the marginal contribution of Energy companies which are likely to be correlated with the business cycle. Energy companies such as Anadarko Ptl. (APC), ConocoPhillips (COP), Occidental Ptl. (OXY), Apache (APA), and Schlumberger (SLB) show now a much lower centrality in the economic network. The magnitude of the median weighted eigenvector centrality for other sectors is relatively low. When aggregate systemic risk is higher (blue line), the weight of Financials tend to dominate other industries. Consistently with the CAPM and the three-factor Fama-French model, financial companies such as JP Morgan (JPM), Bank of America (BAC), Bank of New York Mellon (BK), AIG, Citigroup (C), and Wells Fargo (WFC) are now highly systemically important.

For the sake of completeness, Figure 9 reports the top 20 institutions ranked in both aggregate regimes according to their median eigenvector centrality. The median is computed across posterior simulations of the network structure as provided by equation (14). The red line (blue line) with circle (square) marks shows the centrality measure across companies when aggregate network connectedness is low (high). Top panel shows the ranking computed from the residuals of benchmarking CAPM model. When aggregate network connectivity is low, Energy companies tend to be central for systemic risk management purposes. Exxon Mobil (XOM), Occidental Ptl. (OXY), Schlumberger (SLB), and ConocoPhillips (COP) fills the top of the ranking in terms of centrality within the network. Consistently with top panel of Figure 8 the systemic importance of Financials increases when the network becomes more dense, with JP

Morgan (JPM), Bank of New York (BK) and Bank of America (BAC) bearing most of systemic risk.

[Insert Figure 9 about here]

The same path is confirmed for both the three-factor Fama-French model (mid panel), and the implementation of the I-CAPM model (bottom panel). Interestingly, Figures 8-9 make clear a separation between states of high vs low systemic risks. As a matter of fact, for instance for the three-factor model, the average weighted eigenvector centrality of the top 20 institutions is 0.017 with high systemic risk, against an average median value of 0.0055 when contagion is low. The separation across regimes is robust across factor models and connectivity measures.

4.3.2 Industry-Level Network Centrality. In this section we aggregate the results across sectors to obtain evidences on network centrality at the industry level. Firms are classified in sectors according to the Global Industry Classification Standard (GICS), developed by MSCI. The industry-level centrality measures are obtained by taking the median of firm-specific measures averaged out within industries. For the sake of completeness we report the results computed from both our weighted centrality measure (5) and the standard eigenvector centrality. Figure 10 shows the results. Top left (right) panel shows the results for the weighted eigenvector centrality for the low (high) aggregate network density.

[Insert Figure 10 about here]

As we would expect from firm-level network centrality evidences, both the financial and the energy sector tend to dominates across aggregate systemic risk conditions. Top-right panel shows that when aggregate connectedness is high, the systemic importance of industries such as Utilities, Telecomm, Healthcare, Consumer Staples and Discretionary are almost negligible. This is so as the network is mostly concentrated around few firms of both the financial and the energy sector. Bottom left (right) panel shows the results for the standard eigenvector centrality for the low (high) aggregate systemic risk. The fact that such measure does not take into account the strength of the linkages (i.e. covariance terms), makes other sectors such as Healthcare, Tech and Consumer Staples relatively important for the transmission mechanism of

exogenous shocks. This difference is more evident when considering the regime of low aggregate connectivity (bottom left panel). While the energy sector still makes the top of the ranking in terms of systemic importance, Consumer Staples and Technology now rank second and third, respectively. This makes clear that by weighing existing linkages with covariance terms can lead to have clear cut evidences on the network centrality at the industry level.

4.4 The Relationship with Market Valuations

One may argue that network centrality of a firm/industry is directly linked to its corresponding relative market valuation. The relative weight of the financial sector drops from 20% in 2006 to less than 10% across the great financial crisis of 2008/2009, when network connectedness is high (see Figure 2). This implies an opposite relationship between the centrality of the financial sector and its corresponding market value. The opposite is true for the Energy sector. The relative market value of the energy sector increases across the sample and tend to be high when aggregate connectivity is high as well. The same positive relationship can be seen for Telecommunication Services while Industrial and Materials do not display a clear mapping with aggregate systemic risk. Also, the relative market value of the Technology industry spikes during late 90s and bounce back beginning of 2000. This is the well known dot.com bubble.

We now formally test the existence of any significant relationship between firm-level network centrality and market values across regimes. To this end we estimate a set of univariate cross-sectional regressions where the dependent variable is the centrality measure for each firm in regime k, i.e. $\tilde{x}_{i,k}$, and the independent variable is the corresponding market value averaged across the periods identified by regime k. We compute such regression for each factor pricing model, different regimes and considering both our weighted centrality measure (5) and standard eigenvector centrality. For each regression, we report the regression coefficient, the t-statistic and the adjusted R^2. We also compute a rank-correlation coefficient as in Kendall (1938). We first rank firms according to their centrality within the network, then we rank firms according to their average market value across regimes. The coefficient τ measures the correspondence of the ranking. Table 2 shows the results.

[Insert Table 2 about here]

We find evidence that systemic risk and market value are not correlated. Top panel shows the results for our weighted centrality measure. The delta coefficient is low in magnitude and not statistically significant across regimes. The t-statistics are anywhere below the 5% significance threshold, and the adjusted R^2 is below 2% across models and regimes. Bottom panel shows the results for the standard eigenvector centrality measure. Again, the regression coefficients are low in magnitude and nowhere significant with t-statistics far below the significance threshold. Also, adjusted R^2 reaches the negligible upper bound of 2.3% for network centrality computed from the residuals of an I-CAPM model within the low aggregate connectedness regime. Also, the Kendall (1938) rank-correlation coefficient does not show any sensible mapping between rankings, namely, those firms that are more central to the network does not not have the highest average market value.

5 Systemic Risk and Value Losses

One important implication for any systemic risk measure is its ability to act as an early warning signal for regulators and the public. To this end, we test the null that those firms more exposed to systemic risk are those that tend to experience higher losses, by using a set of cross-sectional regression. For each model and regime we regress the average maximum percentage financial loss (AM%L henceforth) onto the network centrality measure for $i = 1, ..., N$ firms.[8] The results are reported in Table 3 for both out weighted and the standard eigenvector centrality measures.

[Insert Table 3 about here]

Panel A shows the results ranking firms according to the weighted centrality measure (5). We find that companies more exposed to the overall risk of the system, i.e. those with higher weighted eigenvector centrality, are more likely to suffer significant losses when aggregate systemic risk is larger. In this respect, our centrality measure is similar to the marginal expected shortfall (MES) originally proposed by Acharya et al. (2011), which tracks the sensitivity of

[8]Suppose that a regime of high systemic risk lasts from t to $t + h$. The maximum percentage loss for a firm is defined to be the maximum difference between the market capitalization of an institution at time t and $t + h$ dividend by its market capitalization at time t. The average measure is computed by averaging out such maximum percentage loss across those periods identified by the hidden state s_t.

firm ith's return to a system-wide extreme event, thereby providing a market-based measure of firms fragility. Top panel shows that institutions that are more contemporaneously interconnected are those that experience major losses in terms of market valuation. The cross-sectional regression coefficient is significant at standard confidence levels and the adjusted R^2 is around 10% across models. However, such positive correlation between network centrality and market losses is less significant when aggregate connectedness decreases. The results computed from the standard eigenvector centrality measure (Panel B) mainly confirms this patter.

Table 3 also reports a rank-correlation coefficient as in Kendall (1938). We rank firms from 1 to N according to their centrality first and then according to their AM%L suffered across regimes. The rank correlation coefficient τ measures the correspondence of the ranking. The results confirm that there is a significant relationship between network centrality and value losses across firms, especially during periods of high aggregate systemic risk. The rank-correlation coefficients are all significant at the 5% significance level, i.e. more exposed firms will face larger losses on average. This is consistent with previous evidence in Billio et al. (2012), Diebold and Yilmaz (2014) and Ahern (2015).

6 Systemic Risk and the Business Cycle

At the outset of the paper we clarify that we do not take any stake in any particular underlying causal structure of an increasing network connectedness; rather, we take it as given and seek to measure systemic risk from an agnostic point of view. However, understanding systemic risk is of interest to understand financial crisis, and their relationship with the business cycle (see Giglio et al. 2015 for a related discussion).

In this section we take a reduced form approach and investigate if variables which arguably proxy the business cycle are related to systemic risk. Also, we investigate any early warning feature of our aggregate systemic risk probability. We use several macro-financial variables to capture business cycle effects on changes in the investment opportunity set. We consider the term-, default- and credit-yield spreads, the aggregate dividend yield and price-earnings ratio, the VIX index, the Market Uncertainty index proposed by Baker, Bloom, and Davis (2013),

and the Financial Stress Index held by the Federal Reserve Bank of St. Louis.[9]

We formally investigate the relationship between systemic risk and macro-financial variables by estimating a Probit model considering different combinations of the above macro-financial predictors as the set of independent variables Z_t. The dependent variable s_t is the systemic risk state which takes value 1 if the filtered probability of being in a regime of high connectedness is greater than 0.5. First, we consider the contemporaneous relationship between changes in state variables and aggregate systemic risk. Indeed, some of the independent variables such as aggregate dividend yield and default spread are not stationary. Table 4 reports the estimates of the betas and the marginal effect of each independent variable.

[Insert Table 4 about here]

Interestingly, credit and default spreads show a significant explanatory power and are positively correlated with systemic risk, with a pseudo R^2 of 0.03 and 0,12, respectively. Changes to aggregate financial distress are positively (0.424) and significantly (p-value= 0.001) correlated with aggregate network connectivity. As a whole Table 4 shows that credit and default spreads, as well as aggregate financial distress conditions are sensibly and positively correlated with the level of connectedness of the economy as a whole.

7 Conclusions

Systemic risk measurement have become overwhelmingly important over the last few years. After the great financial crisis the main question has been to what extent the economic system is robust to a shock to the financial sector. In the language of network analysis this translates to estimate the connectedness of financial firms with the rest of the economy. We believe we contribute to answer this question by providing a useful and intuitive model for systemic risk measurement.

[9]Default spread is computed as the difference between the yields of long-term corporate Baa bonds and long-term government bonds. The term spread is measured the difference between the yields of 10- and 1-year government bonds. Credit spread is computed as the difference between the yields of long-term Baa corporate bonds and long-term Aaa corporate bonds. Data on bonds, treasuries and financial distress are taken from the FredII database of the Federal Reserve Bank of St.Louis. The data for the 1-month T-Bill are taken from Ibbotson Associates.

We take an asset pricing perspective and infer the network structure system-wide from the residuals of a linear factor pricing model. By conditioning on different sources of systematic risk we implicitly recognize that systematic and systemic risk might be conditional independent but not mutually exclusive. For the sake of completeness we consider different sources of systematic risks such as aggregate financial wealth, size, value and shocks to macroeconomic risk factors.

We estimate the model by developing a Markov Chain Monte Carlo (MCMC) scheme, which naturally embeds parameter uncertainty. This is not a minor advantage. Indeed, in a full information framework any inference on the economic network must be read as contingent on having full confidence in the parameters point estimates. This is rarely the case especially in high dimensional time series settings. Moreover, alternative conceivable values of the parameters will typically lead to different networks. We address this situation by providing an exact finite-sample Bayesian estimation framework which helps generate the posterior distribution of virtually any function of the linear factor model parameters/statistics.

An empirical application on daily returns of a large dimensional set of blue chip stocks, shows that financial firms and sector play indeed a crucial role in systemic risk measurement, beyond their relative market values. Also, we find that companies more exposed to the overall risk of the system, i.e. those with higher weighted eigenvector centrality, are more likely to suffer significant losses when aggregate systemic risk is larger. In this respect, our centrality measure is similar to popular systemic risk measures such as the marginal expected shortfall.

References

Acharya, V., L. Pedersen, T. Phillippon, and M. Richardson. 2011. Measuring Systemic Risk. *Unpublished Working Paper. New York University.* .

Adrian, T., and M. Brunnermeier. 2010. CoVaR. *Unpublished Working Paper. Princeton University and Federal Researve Bank of New York* .

Ahelegbey, D., M. Billio, and R. Casarin. 2014. Bayesian Graphical Models for Structural Vector Autoregressive Processes. *Journal of Applied Econometrics* forthcoming.

Ahern, K. 2015. Network Centrality and the Cross-Section of Stock Returns. *Working Paper* .

Ahren, K., and J. Harford. 2014. The Importance of Industry Links in Merger Waves. *The Journal of Finance* 69:527–576.

Allen, F., and D. Gale. 2000. Financial Contagion. *Journal of Political Economy* 108.

Ang, A., and G. Bekaert. 2002. International asset allocation with regime shifts. *Review of Financial Studies* pp. 1137–1187.

Baker, S., N. Bloom, and S. Davis. 2013. Measuring Economic Policy Uncertainty. *Working Paper* .

Barigozzi, M., and C. Brownlees. 2014. NETS: Network Estimation for Time Series. *Unpublished Working Paper* .

Bekaert, G., M. Ehrmann, M. Fratzscher, and A. Mehl. 2014. Global Crisis and Equity Market Contagion. *Journal of Finance* 6:2597–2649.

Billio, M., M. Getmansky, A. Lo, and L. Pelizzon. 2012. Econometric Measures of Connectedness and Systematic Risk in the Finance and Insurance Sectors. *Journal of Financial Economics* 104:535–559.

Borgatti, S. 2005. Centrality and Network Flow. *Social Networks* 27:55–71.

Brownlees, C., and R. Engle. 2015. SRISK: A Conditional Capital Shortfall Index for Systemic Risk Measurement. *Unpublished Working Paper* .

Brownlees, C., E. Nualart, and Y. Sun. 2014. Realized Networks. *Unpublished Working Paper* .

Campbell, J. 1996. Understanding Risk and Return. *Journal of Political Economy* pp. 298–345.

Campbell, S., and F. Diebold. 2009. Stock returns and expected business conditions: Half a century of direct evidence. *Journal of Business and Economic Statistics* pp. 266–278.

Carter, C., and R. Kohn. 1994. On Gibbs sampling for state-space models. *Biometrika* pp. 541–553.

Carvalho, C., and M. West. 2007. Dynamic Matrix-Variate Graphical Models. *Bayesian Analysis* pp. 69–98.

Carvalho, C., M. West, and H. Massam. 2007. Simulation of Hyper-Inverse Wishart Distributions on Graphical Models. *Biometrika* p. 183.

Casella, G., and C. P. Robert. 2004. *Monte Carlo Statistical Methods*. New York: Springer Verlag.

Chib, S. 1995. Marginal Likelihood from the Gibbs Output. *Journal of the American Statistical Association* 432:1313–1321.

Chib, S., and E. Greenberg. 1995. Hierarchical analysis of SUR models with extensions to correlated serial errors and time-varying parameter models. *Journal of Econometrics* 68:339–360.

Clark, T., and T. Davig. 2011. Decomposing the declining volatility of long-term inflation expectations. *Journal of Economic Dynamics and Control* 35:981–999.

Cochrane, J. 2001. *Asset Pricing*. Princeton, NJ: Princeton University Press.

Corsetti, G., M. Pericoli, and M. Sbracia. 2005. Some Contagion, some Interdependence: More Pitfalls in Tests of Financial Contagion. *Journal of International Money and Finance* 24:1177 – 1199.

Corsetti, G., M. Pericoli, and M. Sbracia. 2011. *Financial Contagion: The Viral Threat to the Wealth of Nations*, chap. Correlation Analysis of Financial Contagion, pp. 11–20. John Wiley & Sons.

Dawid, A., and S. Lauritzen. 1993. Hyper-Markov Laws in the Statistical Analysis of Decomposable Graphical Models. *The Annals of Statistics* pp. 1272–1317.

Dempster, A. 1972. Covariance Selection. *Biometrics* pp. 157–175.

Diebold, F., and K. Yilmaz. 2014. On the Network Topology of Variance Decompositions: Measuring the Connectedness of Financial Firms. *Journal of Econometrics* 182:119–134.

Diebold, F., and K. Yilmaz. 2015. *Financial and Macroeconomic Connectedness: A Network Approach to Measurement and Monitoring*. Oxford University Press.

Easley, D., and J. Kleinberg. 2010. *Networks, Crowds and Markets*. Cambridge University Press.

Emmert-Streib, F., and M. Dehemer. 2012. Exploring Statistical and Population Aspects of Network Complexity. *PLoS ONE* 7(5).

Erdös, P., and A. Rényi. 1959. On the Random Graphs. *Publ. Math.* pp. 290–297.

Fama, E., and K. French. 1993. Common Risk Factors in the Returns on Stocks and Bonds. *Journal of Financial Economics* 33:3–56.

Forbes, K., and R. Rigobon. 2000. *Measuring Contagion: Conceptual and Empirical Issues*. International financial contagion ed. Kluwer Academic Publisher.

Forbes, K., and R. Rigobon. 2002. No Contagion, Only Interdependence: Measuring Stock Market Comovements. *Journal of Finance* pp. 2223–2261.

Frühwirth-Schnatter, S. 1994. Data Augmentation and Dynamic Linear Models. *Journal of Time Series Analysis* 15:183–202.

Frühwirth-Schnatter, S. 2006. *Finite Mixture and Markov Switching Models*. Berlin: Springer-Verlag.

Geman, S., and D. Geman. 1984. Stochastic Relaxation, Gibbs Distributions, and the Bayesian Restoration of Images. *IEEE Transactions* 6:721–741.

Geweke, J. 1992. Evaluating the Accuracy of Sampling-Based Approaches to Calculating Posterior Moments. *Bayesian Statistics 4* .

Giglio, S., B. Kelly, and S. Pruitt. 2015. Systemic Risk and the Macroeconomy: An Empirical Evaluation. *Journal of Financial Economics* forthcoming.

Giudici, P., and P. Green. 1999. Decomposable Graphical Gaussian Model Determination. *Biometrika* 86:758–801.

Goyal, S. 2007. *Connections: An Introduction to the Economics of Networks*. Princeton University Press.

Guidolin, M., and A. Timmermann. 2007. Asset allocation under multivariate regime switching. *Journal of Economic Dynamics and Control* pp. 3502–3544.

Guidolin, M., and A. Timmermann. 2008. International asset allocation under regime switching, skew and kurtosis preferences. *Review of Financial Studies* pp. 889–935.

Hamilton, D., J. 1994. *Time Series Analysis*. Princeton University Press, Princeton.

Hammersley, J., and P. Clifford. 1971. Markov Fields on Finite Graphs and Lattices. *Unpublished Manuscript* .

Hautsch, N., J. Schaumburg, and M. Schienle. 2012. Financial Network Systemic Risk Contributions. *Discussion Paper 2012-053, CRC 649, Humboldt University Berlin* .

Jackson, M. 2008. *Social and Economic Networks*. Princeton University Press.

Jones, B., C. Carvalho, A. Dobra, C. Hans, C. Carter, and M. West. 2005. Experiments in Stochastic Computation for High-Dimensional Graphical Models. *Statistical Science* pp. 388–400.

Justiniano, A., and G. Primiceri. 2008. The Time-Varying Volatility of Macroeconomic Fluctuations. *American Economic Review* 98:604–641.

Kass, R., and A. Raftery. 1995. Bayes Factors. *Journal of the American Statistical Association* 430:773–795.

Kendall, M. 1938. A New Measure of Rank Correlation. *Biometrika* 30:81–89.

Lauritzen, S. 1996. *Graphical Models*. Claredon Press, Oxford.

Liew, J., and M. Vassalou. 2000. Can book-to-market, size and momemtum be risk factors that predict economic growth? *Journal of Financial Economics* pp. 221–245.

Merton, R. 1973. An Intertemporal Capital Asset Pricing Model. *Econometrica* 41:867–887.

Newman, M. 2003. The structure and function of complex networks. *SIAM Review* 45:167–256.

Petkova, R. 2006. Do the Fama-French Factors Proxy for Innovations in Predictive Variables? *Journal of Finance* pp. 581–612.

Primiceri, G. 2005. Time Varying Structural Vector Autoregressions and Monetary Policy. *Review of Economic Studies* 72:821–852.

Roberts, G., and S. Sahu. 1997. Updating schemes, covariance structure, blocking and parametrisation for the Gibbs sampler. *Journal of the Royal Statistical Society* 59:291 – 318.

Tanner, A., and W. Wong. 1987. The Calculation of Posterior Distributions by Data Augmentation. *Journal of the American Statistical Association* 82:528–540.

Timmermann, A., D. Blake, I. Tonks, and A. Rossi. 2014. Network Centrality and Fund Performance. *Working Paper* .

Vassalou, M. 2003. News Related to future GDP growth as a risk factor in equity returns. *Journal of Financial Economics* pp. 47–73.

Wang, H. 2010. Sparse Seemingly Unrelated Regression Modelling: Applications in Finance and Econometrics. *Computational Statistics and Data Analysis* pp. 2866–2877.

Wang, H., and M. West. 2009. Bayesian Analysis of Matrix Normal Graphical Models. *Biometrika* pp. 821–834.

Whittaker, J. 1990. *Graphical Models in Applied Multivariate Statistics*. Chichester, UK: John Wiley and Sons.

Appendix

A The Gibbs Sampler

The completed data likelihood is

$$p\left(\mathbf{y}_{1:T}, \mathbf{s}_{1:T}|\boldsymbol{\theta}, G\right) = \prod_{k,l=1}^{K}\prod_{t=1}^{T}(2\pi)^{-n/2}\left|\tilde{\Sigma}_t\right|^{-n/2}\exp\left(-\frac{1}{2}\left(y_t - X_t'\tilde{\boldsymbol{\beta}}_t\right)'\tilde{\Sigma}_t^{-1}\left(y_t - X_t'\tilde{\boldsymbol{\beta}}_t\right)\right)p_{kl}^{N_{kl,t}} \tag{A.15}$$

with $N_{kl,t} = \mathbb{I}_{\{k\}}\left(s_{t-1}\right)\mathbb{I}_{\{l\}}\left(s_t\right)$. Combining the prior specifications (8)-(11) with the complete likelihood (A.15), we obtain the posterior density

$$p\left(\boldsymbol{\theta}, G, \mathbf{s}_{1:T}|\mathbf{y}_{1:T}\right) \propto p\left(\mathbf{y}_{1:T}, \mathbf{s}_{1:T}|\boldsymbol{\theta}, G\right)p(\boldsymbol{\theta}, G) \tag{A.16}$$

Since the joint posterior distribution is not tractable the Bayesian estimator of the parameters and graphs cannot be obtained in analytical form, thus we approximate the posterior distribution and the Bayes estimator by simulation. The random draws from the joint posterior distributions are obtained through a collapsed multi-move Gibbs sampling algorithm (see e.g. Roberts and Sahu 1997 and Casella and Robert 2004), where the graph structure, the hidden states and the parameter are sampled in blocks. At each iteration the Gibbs sampler sequentially cycles through the following steps:

1. Draw $\mathbf{s}_{1:T}$ conditional on $\boldsymbol{\theta}$, G and $\mathbf{y}_{1:T}$.
2. Draw Σ_k conditional on $\mathbf{y}_{1:T}$, $\mathbf{s}_{1:T}$, G_k and $\boldsymbol{\beta}_k$.
3. Draw G_k conditional on $\mathbf{y}_{1:T}$, $\mathbf{s}_{1:T}$ and $\boldsymbol{\beta}_k$.
4. Draw $\boldsymbol{\beta}_k$ conditional on $\mathbf{y}_{1:T}$, $\mathbf{s}_{1:T}$ and Σ_k.
5. Draw $\boldsymbol{\pi}_k$ conditional on $\mathbf{y}_{1:T}$, $\mathbf{s}_{1:T}$.

A.1 Sampling $\mathbf{s}_{1:T}$

In order to draw the unobservable state at each time and iteration we use a forward filtering backward sampling (FFBS) algorithm (see Frühwirth-Schnatter 1994 and Carter and Kohn 1994). As the state s_t is discrete valued the FFBS is applied in its Hamilton form. The Hamilton filter iterates in two steps, namely prediction and updating. The prediction step at each time t is

$$p\left(s_{t+1} = j|\boldsymbol{\theta}, \mathbf{y}_{1:t}\right) = \sum_{k=1}^{K} p_{kj}p\left(s_t = k|\boldsymbol{\theta}, \mathbf{y}_{1:t}\right) \tag{A.17}$$

The updating step can be easily derived as

$$p(s_{t+1} = j|\boldsymbol{\theta}, \mathbf{y}_{1:t+1}) = \frac{p(\mathbf{y}_{t+1}|s_{t+1} = j, \boldsymbol{\theta}, \mathbf{y}_{1:t})p(s_{t+1} = j|\mathbf{y}_{1:t}, \boldsymbol{\theta})}{p\left(\mathbf{y}_{t+1}|\mathbf{y}_{1:t}, \boldsymbol{\theta}\right)} \tag{A.18}$$

where the normalizing constant is the marginal predictive likelihood defined as

$$p\left(\mathbf{y}_{t+1}|\mathbf{y}_{1:t}, \boldsymbol{\theta}\right) = \sum_{k=1}^{K} p\left(\mathbf{y}_{t+1}|s_{t+1} = k, \boldsymbol{\theta}, \mathbf{y}_{1:t}\right)p\left(s_{t+1} = k|\boldsymbol{\theta}, \mathbf{y}_{1:t}\right) \tag{A.19}$$

The draw $p(\mathbf{s}_{1:T}|\mathbf{y}_{1:T}, \boldsymbol{\theta})$ can then be obtained recursively and backward in time by using the smoothed probabilities as

$$p(\mathbf{s}_{1:T}|\mathbf{y}_{1:T}, \boldsymbol{\theta}) = p\left(s_T|\mathbf{y}_{1:T}, \boldsymbol{\theta}\right)\prod_{t=1}^{T-1} p\left(s_t|s_{t+1}, \mathbf{y}_{1:t}, \boldsymbol{\theta}\right) \tag{A.20}$$

where for instance

$$p\left(s_t = k | s_{t+1} = j, \mathbf{y}_{1:t}, \boldsymbol{\theta}\right) = \frac{p_{kj} p\left(s_t = k | \mathbf{y}_{1:t}, \boldsymbol{\theta}\right)}{p\left(s_{t+1} = j | \theta, \mathbf{y}_{1:t}\right)} \tag{A.21}$$

A.2 Sampling Σ_k

Graphical structuring of multivariate normal distributions is often referred to *covariance selection* modelling (Dempster 1972). In working with covariance selection models, Dawid and Lauritzen (1993) defined a family of Markov probability distributions suitable for covariance matrices on decomposable graphs called *Hyper-Inverse Wishart*. From a Bayesian perspective, for each state $s_t = k$ and graphical structure G_k the hyper-inverse Wishart turns out to be conjugate *locally* (see Carvalho et al. 2007 for a more detailed discussion).

Let $\mathcal{S}_k = \{S_1, \ldots, S_{n_S}\}$ and $\mathcal{P}_k = \{P_1, \ldots, P_{n_P}\}$ be the set of separators and of prime components, respectively, of the graph G_k. By generating the tree representation of the prime components the density of the hyper-inverse Wishart for Σ_k conditional con G_k writes as

$$p(\Sigma_k) = \prod_{j=1}^{n_P} p(\Sigma_{P_j,k}) \prod_{i=1}^{n_S} (p(\Sigma_{S_i,k}))^{-1} \tag{A.22}$$

where

$$p(\Sigma_{P_j,k}) \propto |\Sigma_{P_j,k}|^{-\left(d_k + 2\mathrm{Card}_{(P_j)}\right)/2} \exp\left\{-\frac{1}{2}\mathrm{tr}(\Sigma_{P_j,k}^{-1} D_{k,j})\right\} \tag{A.23}$$

where $D_{P_j,k}$ is the j-th diagonal block of D_k corresponding to $\Sigma_{P_j,k}$.

Let $\mathcal{T}_k = \{t : s_t = k\}$ and $T_k = Card(\mathcal{T}_k)$. By using the sets $\mathcal{S}_k$ and $\mathcal{P}_k$ then the posterior for Σ_k factorizes as follows

$$p\left(\Sigma_k | \mathbf{y}_{1:T}, \boldsymbol{\theta}, \mathbf{s}_{1:T}, \boldsymbol{\beta}_k\right) \propto \tag{A.24}$$

$$\propto \prod_{t=1}^{T} (2\pi)^{-n/2} |\tilde{\Sigma}_t|^{-1/2} \exp\left(-\frac{1}{2}\left(y_t - X_t'\tilde{\boldsymbol{\beta}}_t\right)' \tilde{\Sigma}_t^{-1}\left(y_t - X_t'\tilde{\boldsymbol{\beta}}_t\right)\right) p(\Sigma_k)$$

$$\propto \prod_{t \in \mathcal{T}_k} |\Sigma_k|^{-1/2} \exp\left(-\frac{1}{2}\left(y_t - X_t'\boldsymbol{\beta}_k\right)' \Sigma_k^{-1}\left(y_t - X_t'\boldsymbol{\beta}_k\right)\right) p(\Sigma_k)$$

$$\propto |\Sigma_k|^{-T_k/2} \exp\left(-\frac{1}{2}\sum_{t \in \mathcal{T}_k}\left(y_t - X_t'\boldsymbol{\beta}_k\right)' \Sigma_k^{-1}\left(y_t - X_t'\boldsymbol{\beta}_k\right)\right) p(\Sigma_k)$$

$$\propto \prod_{j=1}^{n_P} |\Sigma_{P_j,k}|^{-T_k/2} \exp\left(-\frac{1}{2}\Sigma_{P_j,k}^{-1}\hat{D}_{P_j,k}\right)$$

$$\prod_{j=1}^{n_P} \propto |\Sigma_{P_j,k}|^{-\left(d_k + 2\mathrm{Card}_{(P_j)}\right)/2} \exp\left\{-\frac{1}{2}\mathrm{tr}(\Sigma_{P_j,k}^{-1} D_{P_j,k})\right\} \tag{A.25}$$

$$\prod_{j=1}^{n_S} \propto |\Sigma_{S_j,k}|^{-\left(d_k + 2\mathrm{Card}_{(S_j)}\right)/2} \exp\left\{-\frac{1}{2}\mathrm{tr}(\Sigma_{S_j,k}^{-1} D_{S_j,k})\right\} \tag{A.26}$$

$$\propto \prod_{j=1}^{n_P} \propto |\Sigma_{P_j,k}|^{-\left(d_k + 2\mathrm{Card}_{(P_j)} + T_k\right)/2} \exp\left\{-\frac{1}{2}\mathrm{tr}(\Sigma_{P_j,k}^{-1}(D_{P_j,k} + \hat{D}_{P_j,k})\right\} \tag{A.27}$$

$$\prod_{j=1}^{n_S} \propto |\Sigma_{S_j,k}|^{-\left(d_k + 2\mathrm{Card}_{(S_j)}\right)/2} \exp\left\{-\frac{1}{2}\mathrm{tr}(\Sigma_{S_j,k}^{-1} D_{S_j,k})\right\} \tag{A.28}$$

$$\propto \mathcal{HIW}_{G_k}\left(d_k + T_k, D_k + \sum_{t \in \mathcal{T}_k} \mathbf{e}_{tk}\mathbf{e}_{tk}'\right) \tag{A.29}$$

where $\hat{D}_{P_j,k}$ is the block of $\hat{D}_k = \sum_{t \in \mathcal{T}_k} \mathbf{e}_{tk}\mathbf{e}_{tk}'$ corresponding to $\Sigma_{P_j,k}$ and $\mathbf{e}_{tk} = \mathbf{y}_t - X_t'\boldsymbol{\beta}_k$.

A.3 Direct Network Search: Sampling G_k

In order to learn the Graph structure G_k conditional on the state k we apply a Markov chain Monte Carlo for multivariate graphical models (see, e.g. Giudici and Green 1999 and Jones et al. 2005). This relies on the computation of the unnormalized posterior over graphs $p_k(G_k|\mathbf{y}_{1:T}, \mathbf{s}_{1:T}) \propto p(\mathbf{y}_{1:T}, s_{1:T}|G_k)p(G_k)$, for any specified state k. It is easy to check that due to the prior independence assumption of the parameters across regimes,

$$p_k\left(\mathbf{y}_{1:T}, \mathbf{s}_{1:T}|G_k\right) = \int\int \prod_{t\in\mathcal{T}_k} (2\pi)^{-n/2} \left|\Sigma_k\right|^{-n/2} \exp\left(\frac{1}{2}\left(y_t - X_t'\boldsymbol{\beta}_k\right)' \Sigma_k^{-1}\left(y_t - X_t'\boldsymbol{\beta}_k\right)\right) p(\boldsymbol{\beta}_k)p(\Sigma|G_k)d\boldsymbol{\beta}_k d\Sigma_k \tag{A.30}$$

This integral cannot be evaluated analytically. We apply a Candidate's formula along the line of Chib (1995) and Wang (2010). Such an approximation gives the value of the marginal likelihood via the identity $p_k\left(\mathbf{y}_{1:T}, \mathbf{s}_{1:T}|G_k\right) = p_k\left(\mathbf{y}_{1:T}, \mathbf{s}_{1:T}, G_k, \boldsymbol{\beta}_k, \Sigma_k\right)/p(\Sigma_k, \boldsymbol{\beta}_k|\mathbf{y}_{1:T}, \mathbf{s}_{1:T})$. As pointed out in Wang (2010), two different approximations may be viable by integrating over disjoint subsets of parameters.

Following Jones et al. (2005) we apply a local-move Metropolis-Hastings based on the conditional posterior $p_k(G_k|\mathbf{y}_{1:T}, \mathbf{s}_{1:T})$. A candidate $G_k^{'}$ is sampled from a proposal distribution $q(G_k^{'}|G_k)$ and accepted with probability

$$\alpha = \min\left\{1, \frac{p_k(G_k^{'}|\mathbf{y}_{1:T}, \mathbf{s}_{1:T})q(G_k|G_k^{'})}{p_k(G_k|\mathbf{y}_{1:T}, \mathbf{s}_{1:T})q(G_k^{'}|G_k)}\right\} = \min\left\{1, \frac{p_k(G_k^{'}|\mathbf{y}_{1:T}, \mathbf{s}_{1:T})p(G_k^{'})q(G_k|G_k^{'})}{p_k(G_k|\mathbf{y}_{1:T}, \mathbf{s}_{1:T})p(G_k)q(G_k^{'}|G_k)}\right\}$$

This add/delete edge move proposal is accurate despite entails a substantial computational burden.

A.4 Sampling $\boldsymbol{\beta}_k$

Conditional on $\mathbf{s}_{1:T}$, Σ_k and G_k, the posterior for the regime-dependent betas $\boldsymbol{\beta}_k$ is conjugate and defined as

$$p\left(\boldsymbol{\beta}_k|\Sigma_k, \mathbf{y}_{1:T}, \mathbf{s}_{1:T}\right) \propto \mathcal{N}_p\left(M_k^*\left(\sum_{t\in\mathcal{T}_k} X_t\Sigma_k^{-1}\left(G_k\right)\mathbf{y}_t + M_k^{-1}\mathbf{m}_k\right), M_k^*\right) \tag{A.31}$$

with $M_k^* = \left(\sum_{t\in\mathcal{T}_k} X_t\Sigma_k^{-1}\left(G_k\right)X_t^{'} + M_k^{-1}\right)^{-1}$, and $\Sigma_k^{-1}\left(G_k\right)$ the inverse of the covariance matrix given the underlying graph structure G_k.

A.5 Sampling the Transition Matrix Π

As regards the transition probabilities $\boldsymbol{\pi}_k = (\pi_{k1}, \ldots, \pi_{kK})$, for the state $s_t = k$, the conjugate Dirichlet prior distribution (8) updates as

$$(\pi_{k1}, \ldots, \pi_{kK}|\mathbf{y}_{1:T}, \mathbf{s}_{1:T}) \sim Dir\left(\delta_{k1} + N_{k1}, \ldots, \delta_{kK} + N_{kK}\right) \tag{A.32}$$

with $N_{kl} = \sum_{t=1}^{T} \mathbb{I}_{\{k\}}\left(s_t\right)\mathbb{I}_{\{l\}}\left(s_{t-1}\right)$ the empirical transition probabilities between the kth and the lth state.

B Testing the Number of Regimes

Our Markov regime-switching factor pricing model outlined in Section 2 implies that network connectivity is state dependent with a finite number of regimes. Economic theory assumes that contagion and firms connectedness is more a shift concept than a steady state justifying our choice of $K = 2$. One may argue, however, that two states are not enough to capture the dynamic features of the network. Therefore, it is sensible to effectively test the null hypothesis of $\mathcal{H}_0 : K = 2$ against the alternative $\mathcal{H}_1 : K = 1, 3$. As usual in the Bayesian literature we based

hypothesis testing on Bayes factors comparing the model with i regimes $\mathcal{M}_i$ against a model with j regimes $\mathcal{M}_j$. Bayes factors are based on marginal likelihoods (see Kass and Raftery 1995); comparing, the two-state vs. the three-state model can be accomplished by computing

$$\mathcal{B}_{ij} = \frac{p(\mathbf{y}_{1:T}|\mathcal{M}_i)p\left(\mathcal{M}_i\right)}{p(\mathbf{y}_{1:T}|\mathcal{M}_j)p\left(\mathcal{M}_j\right)}, \tag{A.33}$$

Marginal likelihoods are computed by integrating out both parameter and state uncertainty;

$$p(\mathbf{y}_{1:T}|\mathcal{M}_i) = \int \sum_{S} p\left(\mathbf{y}_{1:T}|\boldsymbol{\theta}, G, \mathbf{s}_{1:T}; \mathcal{M}_i\right) p\left(\boldsymbol{\theta}, G, \mathbf{s}_{1:T}|\mathbf{y}_{1:T}; \mathcal{M}_i\right) d\boldsymbol{\theta} dG, \tag{A.34}$$

with S and G the set of states and networks, and the posterior distribution $p\left(\boldsymbol{\theta}, G, \mathbf{s}_{1:T}|\mathbf{y}_{1:T}\right)$ obtained from the Gibbs sampler (see Appendix A). Table B.1 shows the marginal likelihoods and corresponding Bayes factors across factor pricing models;

[Insert Table B.1 about here]

The marginal likelihood however, is not available in closed form and can be approximated numerically as in Chib (1995). We assume $p\left(\mathcal{M}_i\right) = p\left(\mathcal{M}_j\right)$. Panel A shows the marginal likelihood is anywhere higher for a model with two regimes. Panel A shows that the empirical evidence provided by Bayes factors in log scale is strongly in favor of a model with two regimes vs. three or one states.

C MCMC Convergence Diagnostics

We report the results of a set of convergence diagnostics of our MCMC algorithm outlined in Section 2 and Appendix A, and with respect to the CAPM specification with $K = 2$. The convergence diagnostics concern the computation a set of inefficiency factors and t-tests for equality of the means across sub-samples of the MCMC chain (see Geweke 1992, Primiceri 2005, Justiniano and Primiceri 2008, and Clark and Davig 2011).

For each individual parameter and latent variable, the inefficiency factor defines the amount of information do we effectively have about the parameters, and is measured as $(1 + 2\sum_{f=1}^{\infty} \rho_f)$, where ρ_f is the f_{th} order auto-correlation of the chain of draws. This inefficiency factor equals the variance of the mean of the posterior draws from the MCMC sampler, divided by the variance of the mean assuming independent draws. If there are some correlation between successive samples, then we might expect that our sample has not revealed as much information of the posterior distribution of our parameter as we could have gotten if the samples draws were independent. As standard in convergence diagnostics, when estimating the inefficiency factor, we use the Bartlett kernel as in Newey and West (1987), with a bandwidth set to 4% of the sample of draws. The inefficiency factor is computed for all the model parameters and applied on a range of choices for the total number of posterior draws as well as burn-in period lengths and thinning for the main model specification. Table C.1 shows the inefficiency factor and the effective sample size for each block of parameters for the CAPM specification;

[Insert Table C.1 about here]

Tables C.1 shows that, for most parameters, the MCMC sampler is rather efficient and requires less than 5000 retained posterior draws to be able to do a reasonably accurate inferential analysis. In case of the time-invariant parameters for the high network connectivity regime the sampler is less efficient. This is likely due to the lower amount of information we have in-sample corresponding to the second state. Nonetheless, the corresponding inefficiency factors suggest on average a minimum number of draws of less than 5000 to achieve an accurate analysis of these parameters. Based on this comparison, we set the number of posterior draws equal to 10000 and thinning value equal to 2, obtaining 5000 draws from the posterior distribution in order to have a fairly satisfactory performance.

We also compute the p-value of the Geweke (1992) t-test for the null hypothesis that the average draws computed with the first 20 percent and last 40 percent of the sample of retained draws are statistically equivalent.

For this particular convergence diagnostic test, we compute the variances of the respective means using the Newey and West (1987) heteroskedasticity and autocorrelation robust variance estimator with a bandwidth set to 4% of the utilized sample sizes. Such test is computed still considering our initial CAPM specification with two states.

[Insert Table C.2 about here]

The convergence diagnostic tests in Table C.2 mainly confirms the efficiency of the MCMC sampler. For example, in the case of the alphas $\boldsymbol{\alpha}_k$ parameters the null hypothesis of equal means across sub-samples of the retained draws is hardly ever rejected at the 5% confidence interval. Thus, inference in the factor model appears to be reasonably accurate when based posterior inference on 10000 draws with a burn-in of 2000 and thin value of 2. Such a choice of the number of draws keeps the computational burden affordable, without penalizing significantly inference precision.

Figure 1. Weighted Network Structure

Example of a weighted network structure. This figure shows the network structure implied by an underlying undirected graphical model. Circles indicate the node and the lines are the edges between nodes. Each dashed circle of the junction tree represents a clique while vertices shared by adjacent nodes of the tree define the separators. In this graph $\{(1,2,3),(4,5,6),(7,8)\}$ is the set of cliques and $\{(2,4)\}$ the separator set. The σ_{ij} covariance terms represents the weights associated to the edges.

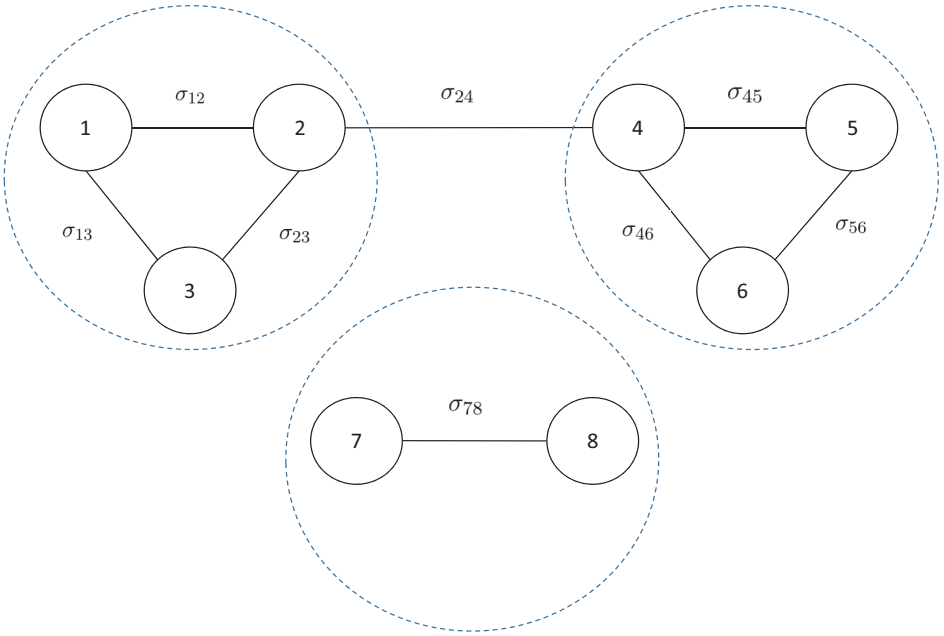

Figure 2. Aggregate Systemic Risk Probability

Systemic Risk Probability. This figure shows the model-implied probability of systemic risk computed from the CAPM (top left), the Fama-French three-factor model (bottom left) and the I-CAPM implementation with default-, term-spread and the aggregate dividend yield in addition to aggregate wealth as risk factors. The gray area represents the systemic risk probability, while the blue line shows the NBER recession indicator for the period following the peak of the recession to the through. Bottom-right panel shows the transition probabilities across models. The first (last) three columns represent the probability of staying in a state of low (high) systemic risk. Transition probabilities are computed for the three-factor Fama-French model, the CAPM and an I-CAPM implementation, respectively. The sample period is 05/10/1996-10/31/2014, daily.

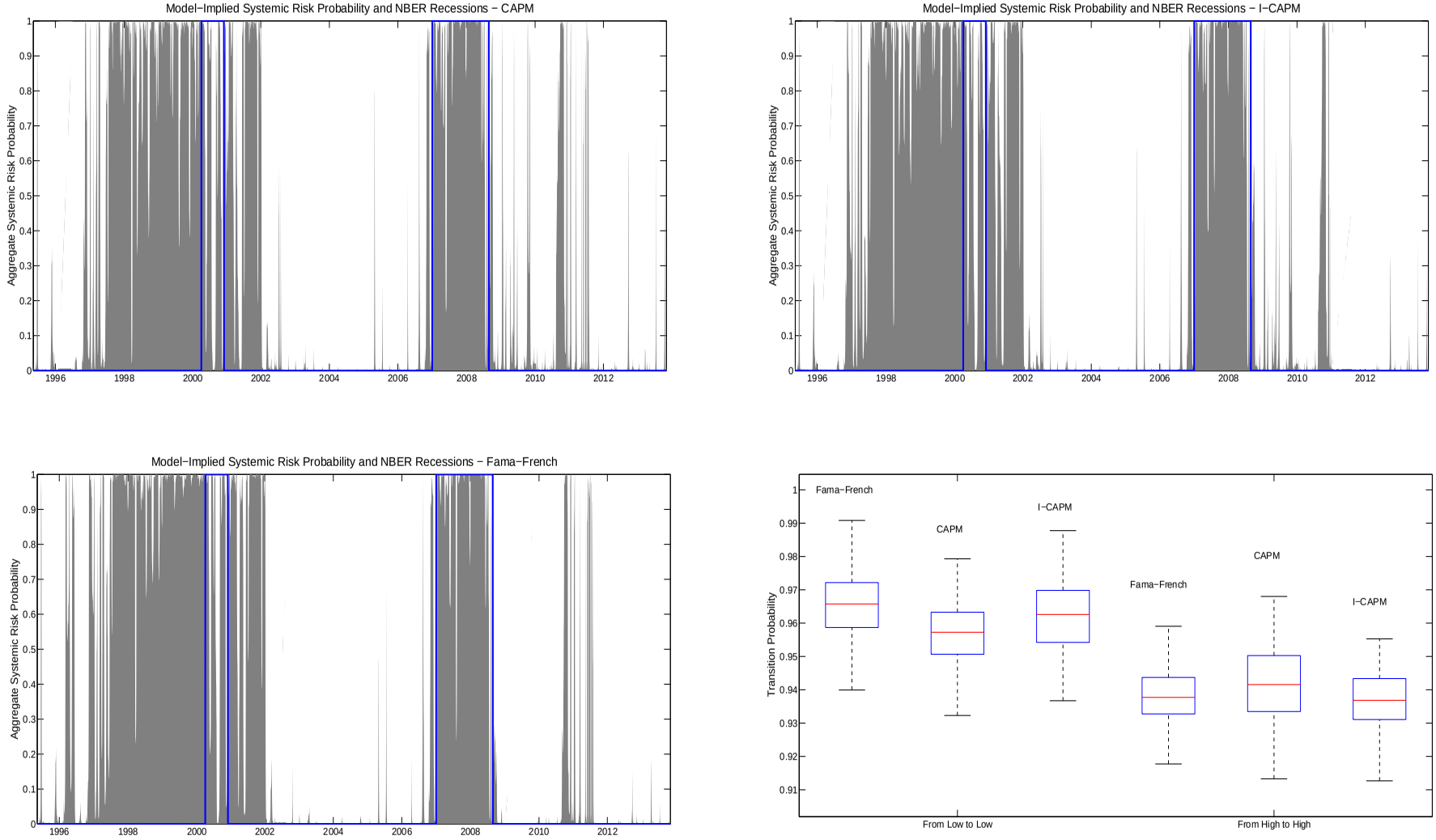

Figure 3. Changes in Exposures to Systematic Risks - Low vs High Systemic Risk, Three-Factor Model

Conditional alphas and betas. This figure reports changes in the conditional intercepts and exposures to sources of systematic risks for each of the stock in the sample. Top left panel shows the so-called Jensen's alpha. Top right panel reports the exposure to market risk (excess return on aggregate wealth). Bottom left and right panel report the firms exposures on the size and value effects as originally proposed in Fama and French (1993). The sample period is 05/10/1996-10/31/2014, daily.

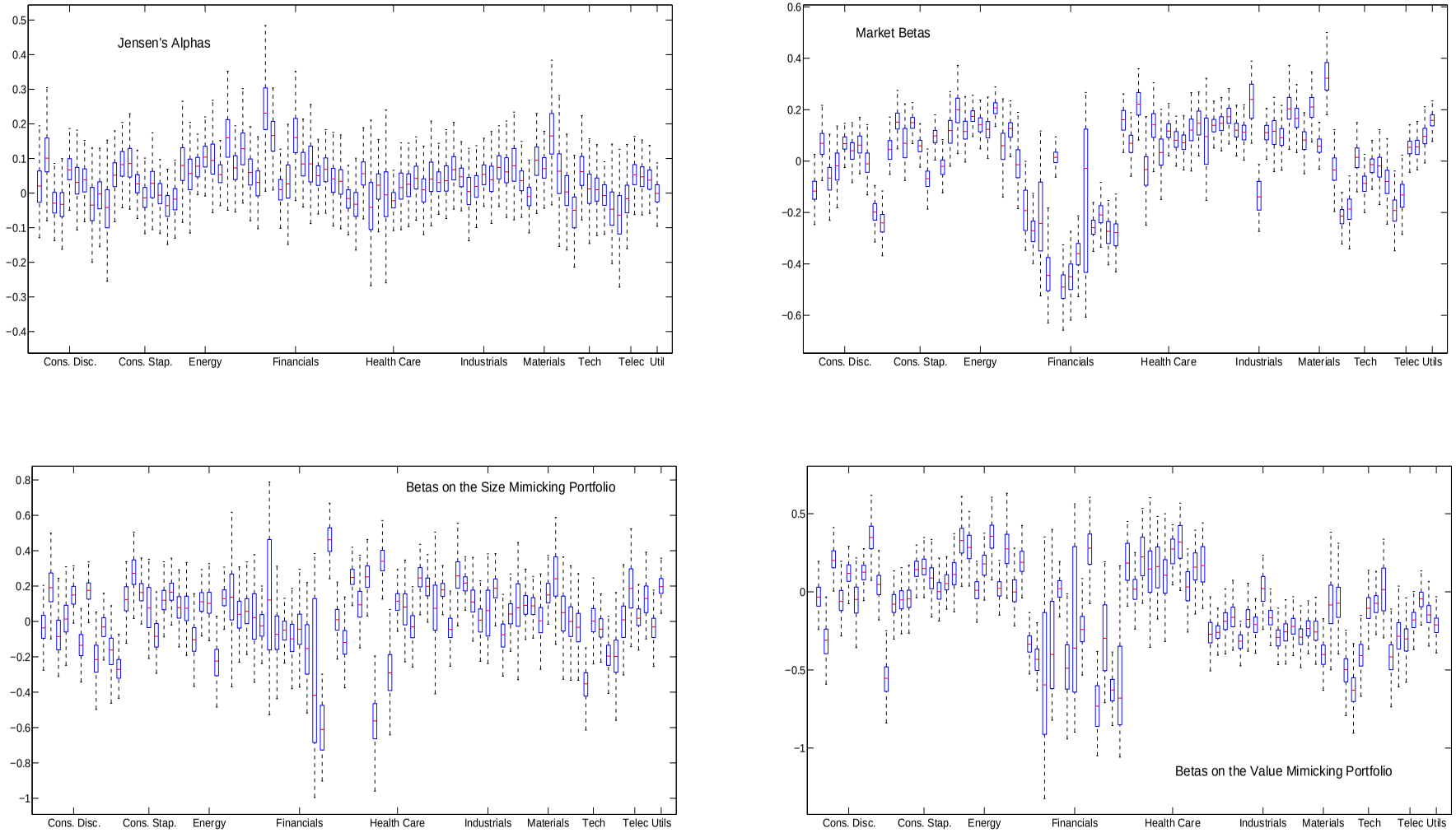

Figure 4. Changes in Exposures to Systematic Risks - Low vs High Systemic Risk, I-CAPM

Conditional alphas and betas. This figure reports the changes to conditional intercepts and exposures to sources of systematic risks for each of the stock in the sample. Top left panel shows the so-called Jensen's alpha. Top right panel reports the exposure to market risk (excess return on aggregate wealth). Bottom left and right panel report the firms exposures on the default and aggregate dividend yield. The sample period is 05/10/1996-10/31/2014, daily.

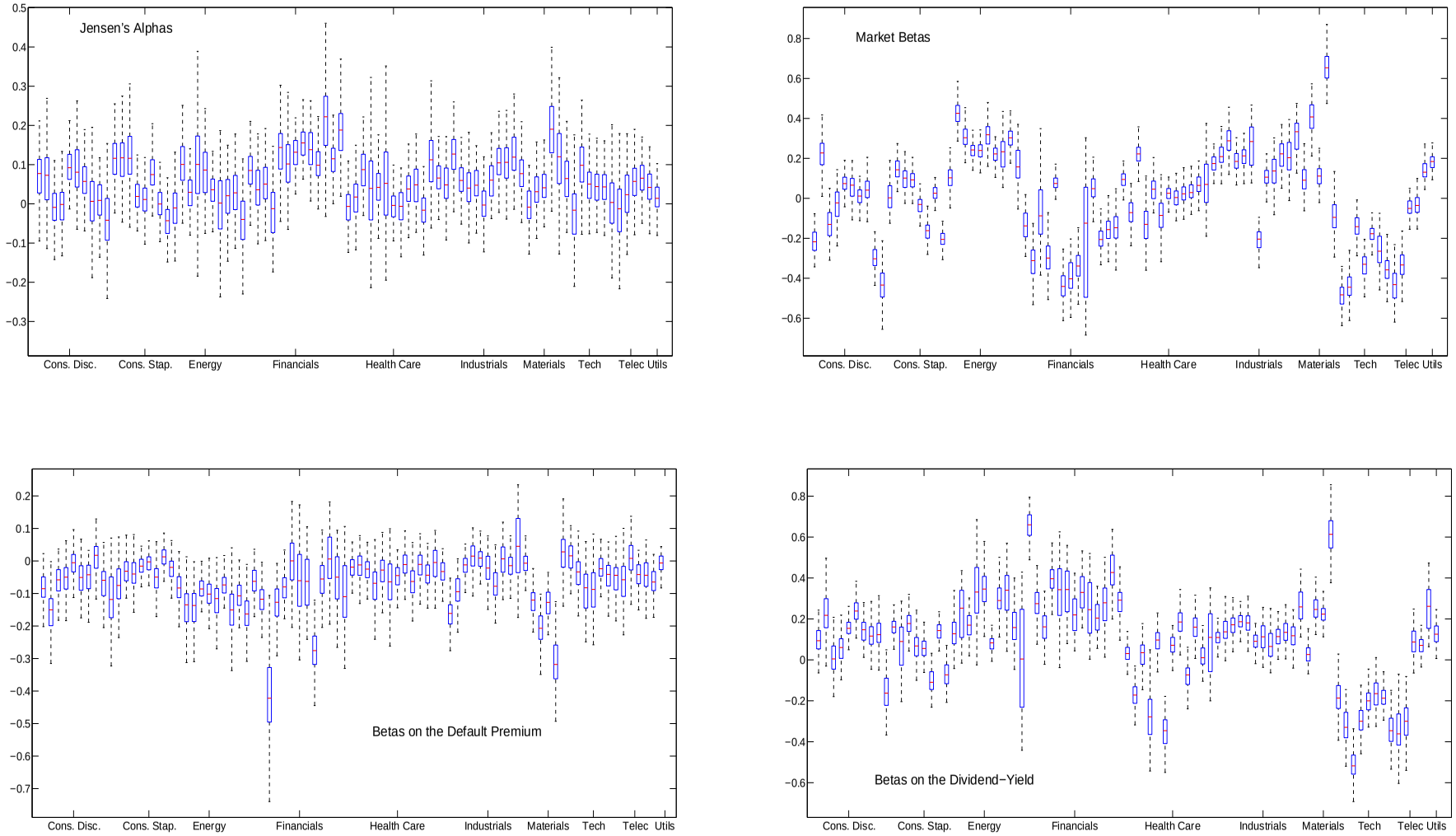

Figure 5. Weighted Network Connectedness: CAPM

Network connectivity conditioning for market risk. This figure report the network structure computed conditioning for market risk. Top panel shows the network connectedness when systemic risk, or contagion, is low. Bottom panel shows the structure of the network when systemic risk increases.

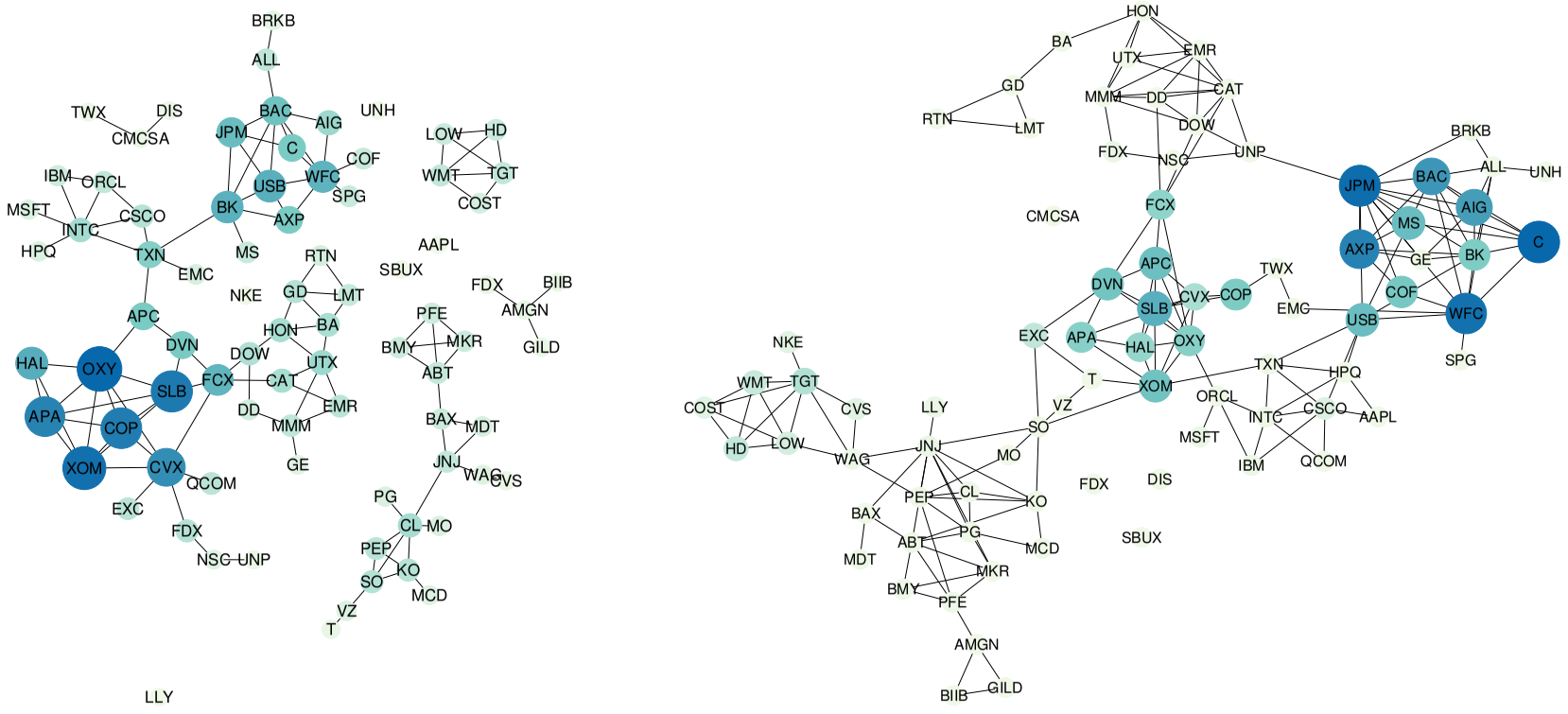

(a) Low Systemic Risk

(b) High Systemic Risk

Figure 6. Weighted Network Connectedness: Three-Factor Model

Network connectivity conditioning for market risk, size and value. This figure reports the network structure computed conditioning for additional sources of systematic risk such as size and value. Top panel shows the network connectedness when systemic risk, or contagion, is low. Bottom panel shows the structure of the network when systemic risk increases.

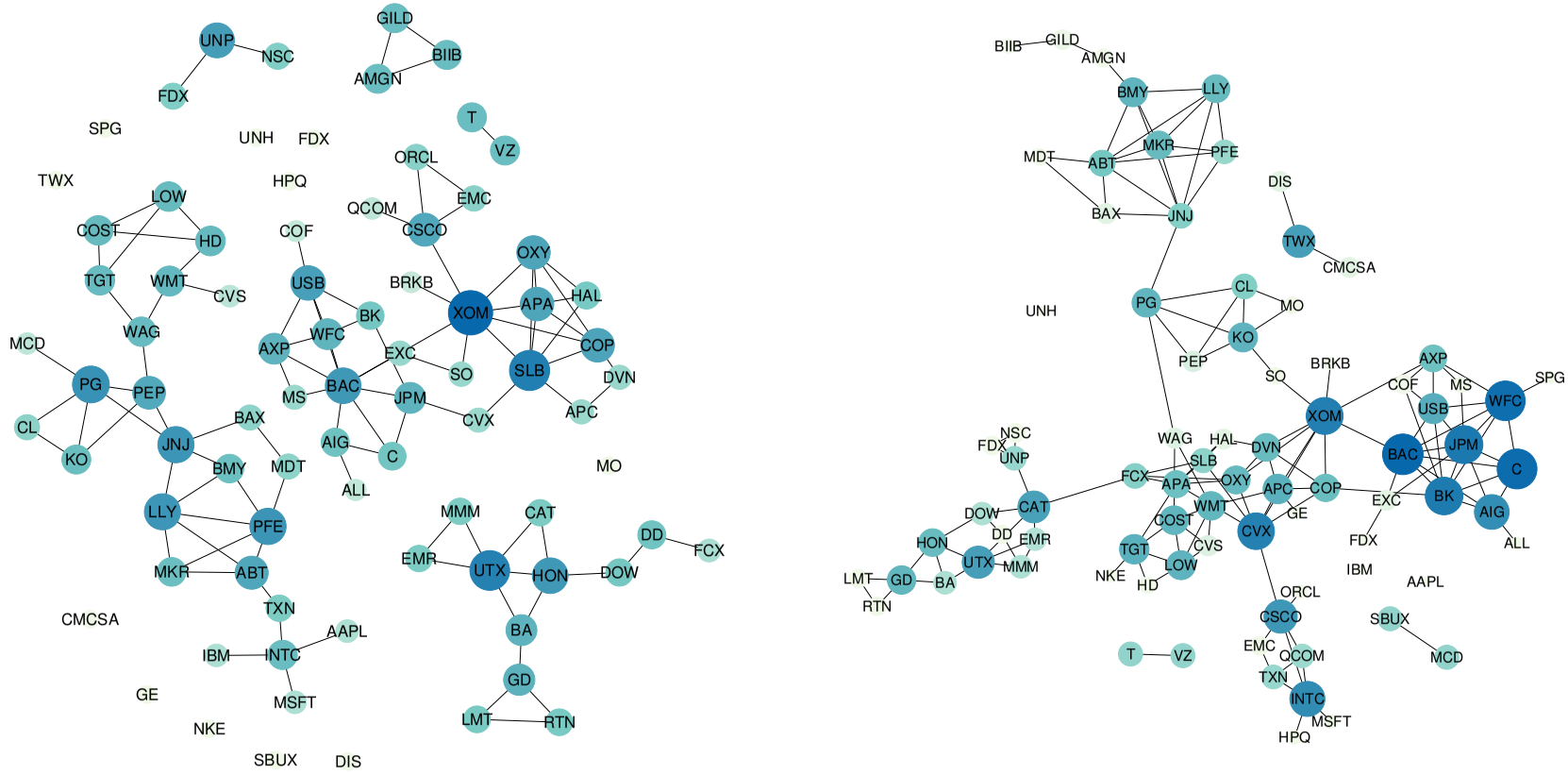

(a) Low Systemic Risk

(b) High Systemic Risk

Figure 7. Weighted Network Connectedness: I-CAPM

Network connectivity from an I-CAPM implementation. This figure reports the network structure computed conditioning for additional sources of systematic risk such as default and term spread, and aggregate dividend yield. Top panel shows the network connectedness when systemic risk, or contagion, is low. Bottom panel shows the structure of the network when systemic risk increases.

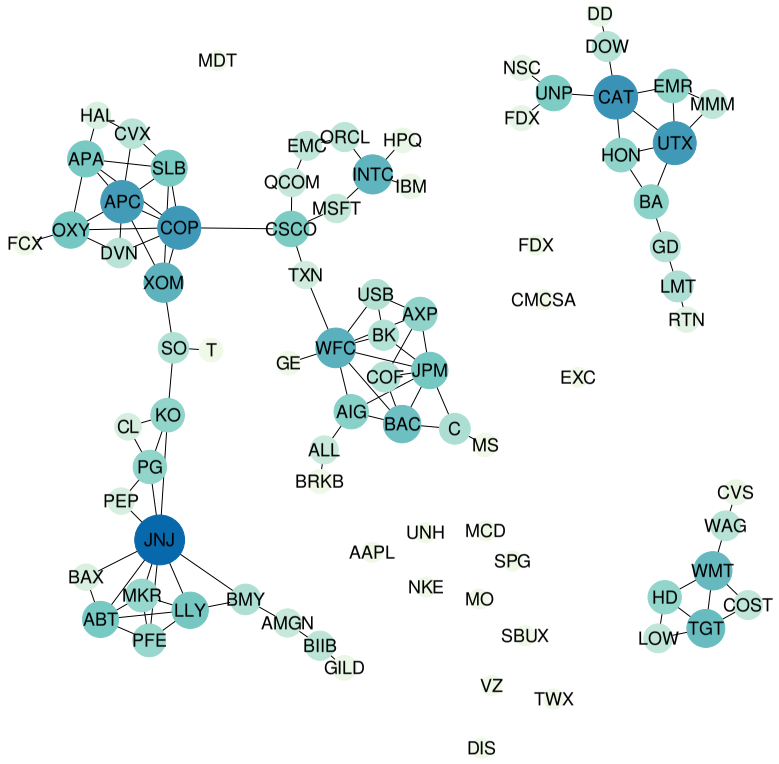

(a) Low Systemic Risk

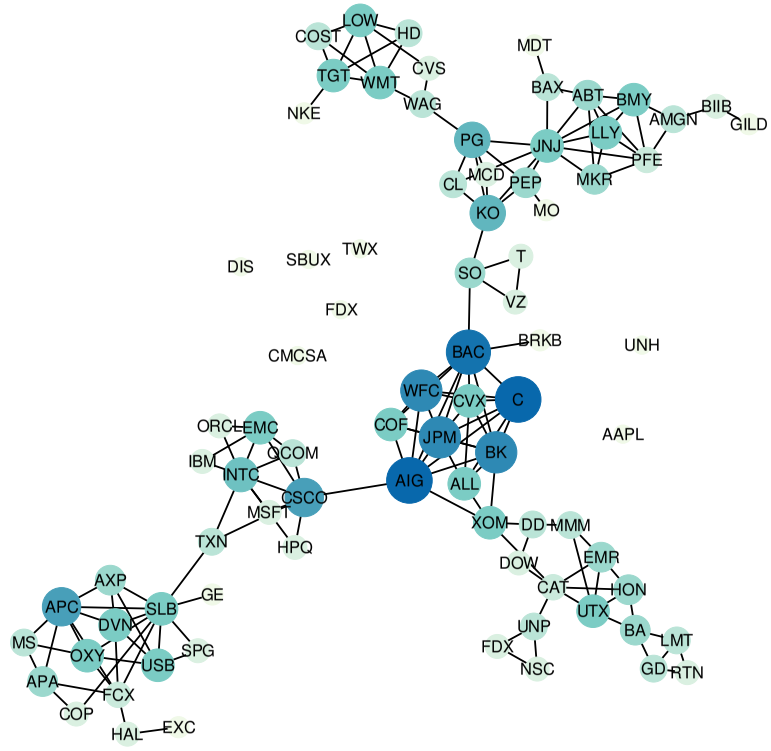

(b) High Systemic Risk

Figure 8. Weighted Eigenvector Centrality

Weighted eigenvector centrality, median values. This figure plots the median weighted eigenvector centrality sorted for the top 20 institutions for both low and high systemic risk. The weighted eigenvector centrality measures the systemic importance of each industry within the economic network, incorporating the strength of the linkages measured by the covariances. The sample period is 05/10/1996-10/31/2014, daily. The network structure is computed conditioning on aggregate wealth (CAPM, top panel), then adding size and value risk fators (Fama-French, mid panel), and conditioning on shocks to financial state variables (I-CAPM, bottom panel).

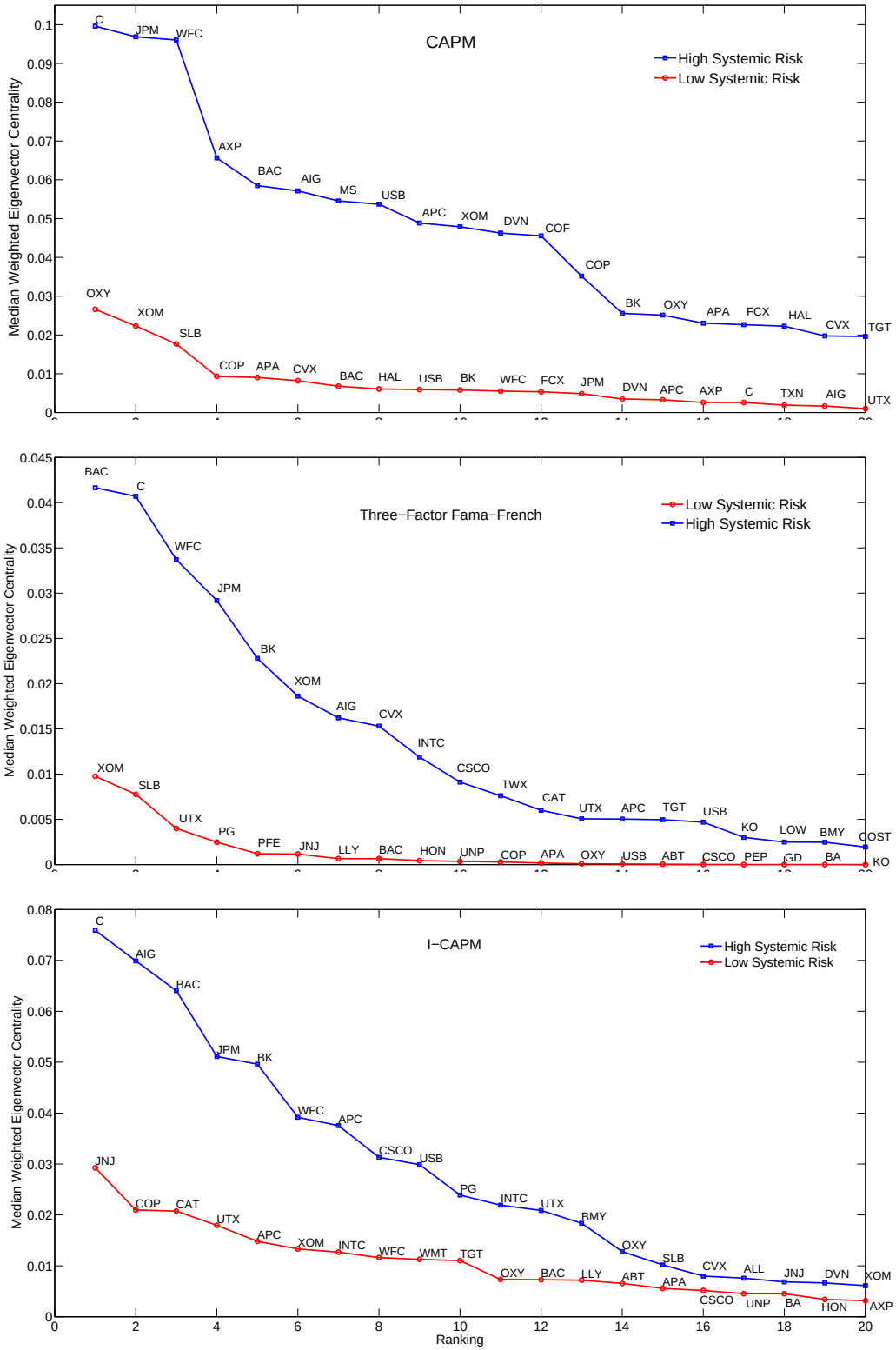

Figure 9. Standard Eigenvector Centrality

Eigenvector centrality, median values. This figure plots the median eigenvector centrality sorted for the top 20 institutions for both low and high systemic risk. Standard eigenvector centrality measures the systemic importance of each industry within the economic network. The sample period is 05/10/1996-10/31/2014, daily. The network structure is computed conditioning on aggregate wealth (CAPM, top panel), then adding size and value risk fators (Fama-French, mid panel), and conditioning on shocks to macro-finance state variables (I-CAPM, bottom panel).

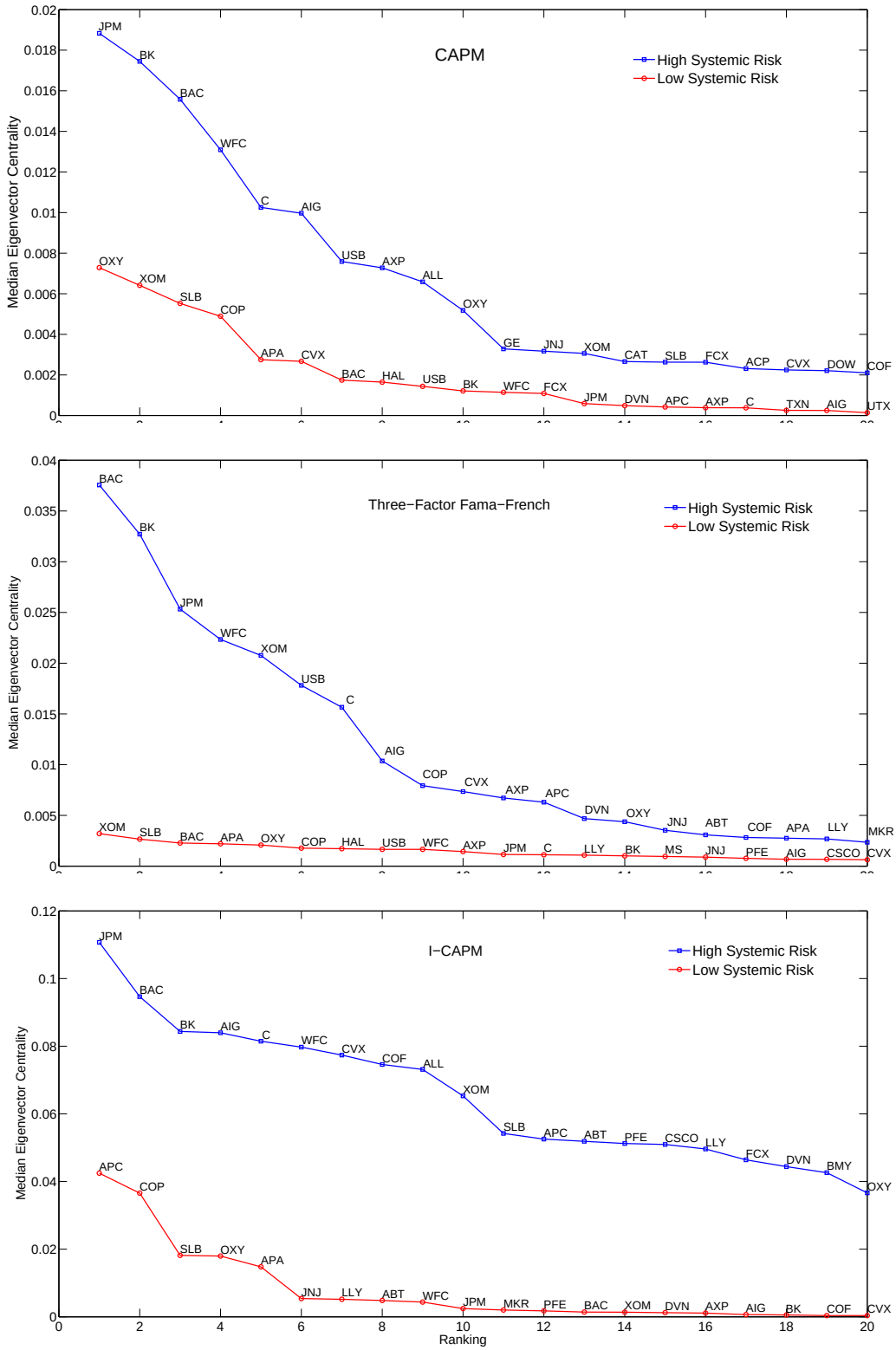

Figure 10. Weighted and Standard Eigenvector Centrality at the Industry Level

Centrality measures across industries. This figure plots the median weighted (top panels) and standard (bottom panels) eigenvector centrality averaged out within industries for both low (left column) and high (right column) regimes of systemic risk. Standard eigenvector centrality measures the systemic importance of each industry within the economic network. The weighted eigenvector centrality incorporates the strength of the linkages measures by the covariances. Industry classification is based on the Global Industry Classification Standard (GICS) developed by MSCI. The sample period is 05/10/1996-10/31/2014, daily. The network structure is computed conditioning on aggregate wealth (CAPM), then adding size and value risk fators (Fama-French), and conditioning on shocks to macro-finance state variables (I-CAPM).

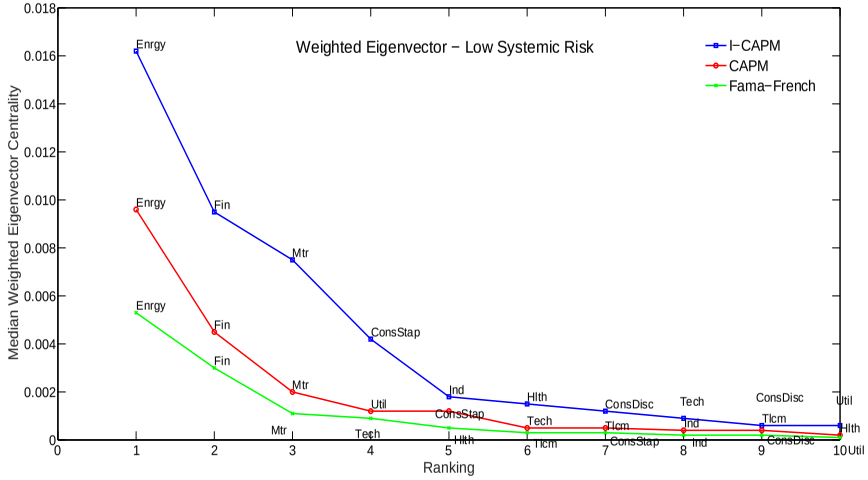

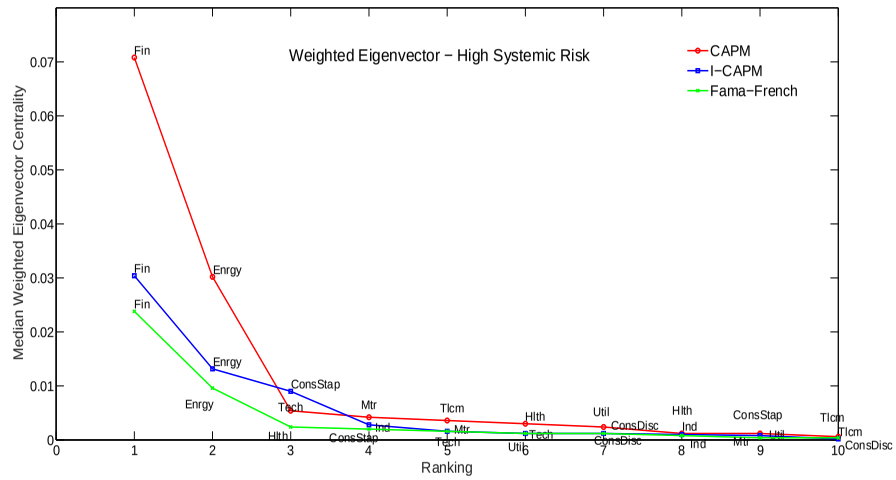

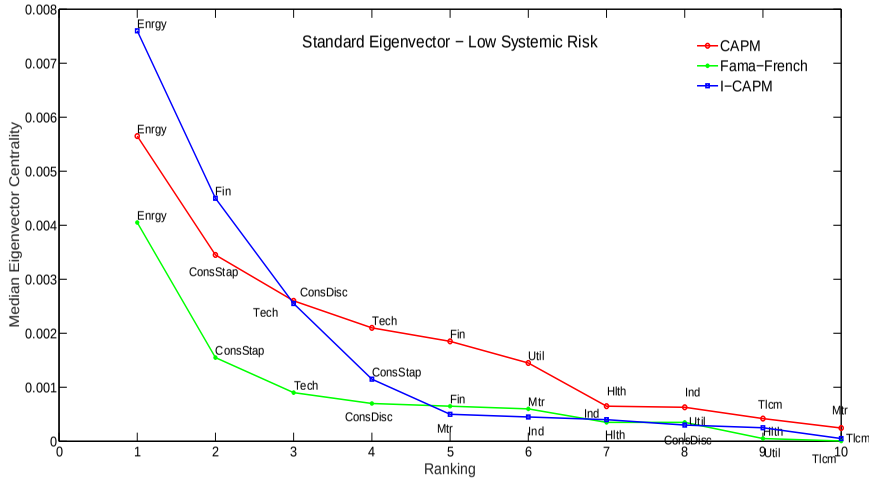

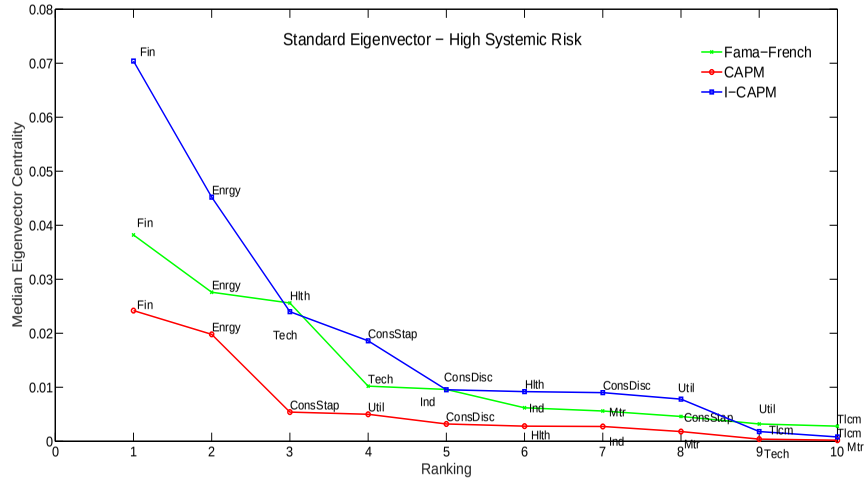

Table 1. Company List

This table summarize the companies in our dataset and the corresponding industry classification according to the Global Industry Classification Standard (GICS), developed by MSCI. These companies represent the subset of the blue chip stocks constitute the S&P100 for which we have at least 15 years of daily data. The S&P100 composition listing is taken as of December 2014.

ID	Ticker	Company Name	GICS Sector	ID	Ticker	Company Name	GICS Sector
1	MMM	3M	Industrials	42	HAL	Halliburton	Energy
2	T	AT&T	Tel. Services	43	HPQ	Hewlett-Packard	Technology
3	ABT	Abbot Labs	Health Care	44	HD	Home Depot	Cons. Disc
4	ALL	All State	Financials	45	HON	Honeywell Intl	Industrials
5	MO	Altria Group	Cons. Stap.	46	INTC	Intel	Technology
6	AXP	American Exp	Financials	47	IBM	International Bus Mchs	Technology
7	AIG	American Intl Gp.	Financials	48	JPM	JP Morgan Chase	Financials
8	AMGN	Amgen	Health Care	49	JNJ	Johnson & Johnson	Health Care
9	APC	Anadarko Petroleum	Energy	50	LLY	Eli Lilly	Health Care
10	APA	Apache	Energy	51	LMT	Lockheed Martin	Industrials
11	AAPL	Apple	Technology	52	LOW	Lowe's Comp.	Cons. Disc
12	BAC	Bank of America	Financials	53	MCD	McDonald's	Cons. Disc
13	BAX	Baxter Intl	Health Care	54	MDT	Medtronic	Health Care
14	BRKB	Berkshire Hathaway	Financials	55	MKR	Merck & Company	Health Care
15	BIIB	Biogen Idec	Health Care	56	MSFT	Microsoft	Technology
16	BA	Boeing	Industrials	57	MS	Morgan Stanley	Financials
17	BMY	Bristol Myers Squibb	Health Care	58	NKE	Nike	Cons. Disc
18	CVS	CVS Health	Cons. Stap.	59	NSC	Norfolk Southern	Industrials
19	COF	Capital One Finl.	Financials	60	OXY	Occidential Plt.	Energy
20	CAT	Caterpillar	Industrials	61	ORCL	Oracle	Technology
21	CVX	Chevron	Energy	62	PEP	PepsiCo	Cons. Disc
22	CSCO	Cisco System	Technology	63	PFE	Pfizer	Health Care
23	C	Citigroup	Financials	64	PG	Procter & Gamble	Cons. Stap.
24	KO	Coca Cola	Cons. Stap.	65	QCOM	Qualcomm	Technology
25	CL	Colgate-Palm.	Cons. Stap.	66	RTN	Raytheon	Industrials
26	CMCSA	Comcast	Cons. Disc	67	SLB	Schlumberger	Energy
27	COP	ConocoPhillips	Energy	68	SPG	Simon Property Grp.	Financials
28	COST	Costco	Cons. Stap.	69	SO	Southern	Utilities
29	DVN	Devon Energy	Energy	70	SBUX	Starbucks	Cons. Disc
30	DOW	Dow Chemical	Materials	71	TGT	Target	Cons. Disc
31	DD	DuPont	Materials	72	TXN	Texas Instruments	Technology
32	EMC	EMC	Technology	73	BK	Bank of New York Mellon	Financials
33	EMR	Emerson Elect.	Industrials	74	TWX	Time Warner	Cons. Disc.
34	EXC	Exelon	Utilities	75	USB	US Bancorp	Financials
35	XOM	Exxon Mobil	Energy	76	UNP	Union Pacific	Industrials
36	FDX	Fedex	Industrials	77	UTX	United Tech	Industrials
37	F	Ford Motor	Cons. Disc	78	UNH	UnitedHealth Grp	Health Care
38	FCX	Freeport-McMoran	Materials	79	VZ	Verizon	Tel. Services
39	GD	General Dynamics	Industrials	80	WMT	WalMart	Cons. Stap.
40	GE	General Electric	Industrials	81	WAG	Walgreen	Cons. Stap.
41	GILD	Gilead Sciences	Health Care	82	DIS	Walt Disney	Cons. Disc.
				83	WFC	Wells Fargo	Financials

Table 2. Network Centrality and Market Values

Centrality measures and market value. This table report the results from a robust regression analysis where the dependent variable is the centrality measure computed for each firm. The independent variable is the company specific corresponding market value. The regression is run for both regimes of systemic risk. Kendall (1938) rank-correlation coefficient is computed by first ranking firms according to their centrality within the network. Second we rank firms according to their average market value across the identified regimes. The rank correlation coefficient τ measures the correspondence of the ranking. Panel A shows the results obtained using the median weighted centrality measure as dependent variable. Panel B shows the results obtained using the median standard centrality measure as dependent variable. Standard errors are corrected for heteroskedasticity and autocorrelation in the residuals (Newey-West HAC). Rank-correlation that are significant at the 5% significance level are displayed in bold.

Panel A: Weighted Eigenvector Centrality

	CAPM				Fama-French				I-CAPM			
	Coeff	t-stat	R^2	τ	Coeff	t-stat	R^2	τ	Coeff	t-stat	R^2	τ
High	0.012	0.908	0.002	0.054	0.001	0.649	0.001	0.061	0.011	0.654	0.003	0.045
Low	0.015	1.072	0.016	**0.084**	0.041	0.871	0.006	**0.085**	0.032	1.032	0.004	0.055

Panel B: Standard Eigenvector Centrality

	CAPM				Fama-French				I-CAPM			
	Coeff	t-stat	R^2	τ	Coeff	t-stat	R^2	τ	Coeff	t-stat	R^2	τ
High	0.099	0.861	0.011	0.062	0.003	0.123	0.003	0.059	0.021	0.782	0.012	0.048
Low	0.021	1.592	0.021	**0.091**	0.002	0.231	0.008	**0.085**	0.042	1.321	0.023	0.052

Table 3. Network Centrality and Value Losses

Value losses and exposure to systemic risk. This table report the results from a robust regression analysis where the dependent variable is the ranking of firms on the basis of their average maximum percentage financial loss suffered across the two separate regimes. The independent variables are the network centrality measures explained in Section 2. Kendall (1938) rank-correlation coefficient is computed by first ranking firms according to their centrality within the network. Second we rank firms according to their average maximum percentage financial loss. The rank correlation coefficient τ measures the correspondence of the ranking. Panel A shows the results obtained using the median weighted centrality measure as dependent variable. Panel B shows the results obtained using the median standard centrality measure as dependent variable. Standard errors are corrected for heteroskedasticity and autocorrelation in the residuals (Newey-West HAC). Rank-correlation that are significant at the 5% significance level are displayed in bold.

Panel A: Weighted Eigenvector Centrality

	CAPM				Fama-French				I-CAPM			
	Coeff	t-stat	R^2	τ	Coeff	t-stat	R^2	τ	Coeff	t-stat	R^2	τ
High	0.551	2.061	0.091	**0.211**	0.671	2.194	0.101	**0.205**	0.891	1.981	0.112	**0.198**
Low	0.213	1.651	0.045	**0.181**	0.391	1.691	0.062	**0.171**	0.691	1.759	0.061	**0.169**

Panel B: Standard Eigenvector Centrality

	CAPM				Fama-French				I-CAPM			
	Coeff	t-stat	R^2	τ	Coeff	t-stat	R^2	τ	Coeff	t-stat	R^2	τ
High	0.421	1.951	0.078	**0.191**	0.671	1.981	0.083	**0.198**	0.521	1.931	0.08	**0.185**
Low	0.172	1.761	0.055	**0.188**	0.401	1.641	0.051	**0.185**	0.301	1.761	0.054	**0.160**

Table 4. Network Connectivity and Changes in Macro-Financial Variables

Systemic risk and changes in standard predictors. This table report the results from a Probit regression analysis where the dependent variable is the model implied systemic risk indicator s_t. The set of independent variables are *changes* from $t-1$ to t of the term yield spread (TERM, the difference between the 10-year interest rate and the 1-month T-Bill rate), the default spread (DEF, the difference between the 30-year treasury yield and the yield on a Baa corporate bond), the aggregate market dividend yield (DY), the credit spread (Credit, the difference between the Baa and the Aaa corporate bond yields), the financial distress index (Distress, a synthetic indicator of financial distress in the U.S.), the aggregate price-earnings ratio (PE), the market uncertainty index (Mkt Unc) from Baker et al. (2014), and the VIX index. Data are from the FredII database of the St Louis Fed and the Chicago Board Options Exchange (CBOE). The sample period is 05/10/1996-10/31/2014, daily. Panel A shows the estimated betas and Panel B the marginal effects. ***means statistical significance at the 1% confidence level, ** significance at the 5% confidence level and * significance at the 10% level.

Panel A: Betas											
	M1	M2	M3	M4	M5	M6	M7	M8	M9	M10	M11
Intercept	-0.335^{***}	-0.332^{***}	-0.335^{***}	-0.334^{***}	-0.334^{***}	-0.332^{***}	-0.325^{***}	-0.332^{***}	-0.335^{***}	-0.335^{***}	-0.330^{***}
Term	0.656^{***}								0.738^{***}	0.701^{***}	
Credit		2.321^{***}								2.451^{***}	
Default			1.998^{***}						2.147^{***}		
DY				0.306					0.891		
PE					-0.021					-0.067	
VIX						-0.002			-0.012	-0.006	0.001
Distress							0.424^{***}				
Mkt Unc								0.001			-0.002
Pseudo R^2	0.01	0.03	0.12	0.01	0.01	0.02	0.09	0.01	0.14	0.15	0.01

Panel B: Marginal Effects											
	M1	M2	M3	M4	M5	M6	M7	M8	M9	M10	M11
Term	0.248								0.281	0.264	
Credit		0.875								0.927	
Default			0.798						0.812		
DY				0.115					0.336		
PE					-0.008					-0.025	
VIX						-0.001			-0.005	-0.002	0.001
Distress							0.261				
Mkt Unc								0.001			-0.001

Table B.1. Testing the Number of Regimes

Testing the number of regimes. This table reports the results of a formal test for the number of regimes for each factor pricing model specification. We report the (log) marginal likelihoods and the corresponding Bayes factor in log-scale comparing the model with $K = 1, 2, 3$. The sample period is 05/10/1996-10/31/2014, daily.

Panel A: Log Marginal Likelihoods			
	CAPM	Fama-French	I-CAPM
$K = 1$	$-1.84e+06$	$-1.86e+06$	$-1.87e+06$
$K = 2$	$-1.75e+05$	$-1.63e+05$	$-1.56e+05$
$K = 3$	$-1.60e+06$	$-1.62e+06$	$-1.63e+06$
Panel B: Log_{10} Bayes Factors			
	CAPM	Fama-French	I-CAPM
$\mathcal{B}_{2,3}$	6.2223	6.2302	6.2346
$\mathcal{B}_{2,1}$	6.1547	6.1632	6.1680

Table C.1. Inefficiency Factors

The table summarizes the convergence results, for the posterior values of the model parameters. The sample period is 05/10/1996-10/31/2014, daily. The estimated inefficiency factors are based on the Bartlett kernel as in Newey and West (1987) with a bandwidth equal to 4% of the 10000 retained draws. Panel A shows the inefficiency factor. This measures define the amount of information do we effectively have about the parameters.

	Parameters	Mean	Median	Min	Max	5%	95%
$\boldsymbol{\alpha}_1$	83	2.9191	2.9299	2.4766	3.5318	2.6046	3.3032
$\boldsymbol{\alpha}_2$	83	3.7976	3.8472	2.4247	6.6805	2.8534	5.3942
$\boldsymbol{\beta}_1$	83	2.1821	7.1531	2.5054	9.9405	2.6542	14.9968
$\boldsymbol{\beta}_2$	83	4.0833	7.1225	2.7312	13.3890	3.1195	11.0579

Table C.2. Testing Differences in Sample Means

The table summarizes the convergence results, for the posterior values of the model parameters. For each of these, we compute the p-value of the Geweke (1992) t-test for the null hypothesis of equality of the means computed for the first 20% and the last 40% of the retained 5000 draws. The variances of the means are estimated with the Newey and West (1987) variance estimator using a bandwidth of 4% of the respective sample sizes.

	Parameters	5% Reject Rate	10% Reject Rate
$\boldsymbol{\alpha}_1$	83	0.0057	0.0093
$\boldsymbol{\alpha}_2$	83	0.0083	0.0113
$\boldsymbol{\beta}_1$	83	0.0101	0.0145
$\boldsymbol{\beta}_2$	83	0.0123	0.0167